Organic Electronics 15 (2014) 667–674

Contents lists available at ScienceDirect

Organic Electronics

journal homepage: www.elsevier.com/locate/orgel

Green and blue–green light-emitting electrochemical cells based on cationic iridium complexes with 2-(4-ethyl-2-pyridyl)-1H-imidazole ancillary ligand

Chozhidakath Damodharan Sunesh [a], George Mathai [b], Youngson Choe [a,*]

[a] Department of Polymer Science and Chemical Engineering, Pusan National University, Busan 609-735, South Korea
[b] Department of Chemistry, Sacred Heart College, Thevara, Kochi 682 013, India

ARTICLE INFO

Article history:
Received 6 November 2013
Received in revised form 9 December 2013
Accepted 21 December 2013
Available online 7 January 2014

Keywords:
Light-emitting electrochemical cells
Iridium complexes
Blue–green emission
Electrochemical properties
Electroluminescence

ABSTRACT

The ionic iridium complexes, $[Ir(ppy)_2(EP\text{-}Imid)]PF_6$ (Complex 1) and $[Ir(dfppy)_2(EP\text{-}Imid)]PF_6$ (Complex 2) are used as the light-emitting material for the fabrication of light-emitting electrochemical cells (LECs). These complexes have been synthesized, employing 2-(4-ethyl-2-pyridyl)-1H-imidazole (EP-Imid) as the ancillary ligand, 2-phenylpyridine (ppy) and 2-(2,4-difluorophenyl)pyridine (dfppy) as the cyclometalated ligands, which were characterized by various spectroscopic, photophysical and electrochemical methods. The photoluminescence (PL) emission spectra in acetonitrile solution show blue–green and blue light emission for Complexes 1 and 2 respectively. However, LECs incorporating these complexes resulted in green (522 nm) light emission for Complex 1 with the Commission Internationale de L'Eclairage (CIE) coordinates of (0.33, 0.56) and blue–green (500 nm) light emission for Complex 2 with the CIE coordinates of (0.24, 0.44). Using Complex 1, a maximum luminance of 1191 cd m^{-2} and current efficiency of 1.0 cd A^{-1} are obtained while that of Complex 2 are 741 cd m^{-2} and 0.88 cd A^{-1} respectively.

1. Introduction

Light-emitting electrochemical cells (LECs) are the next generation solid-state lighting devices which employ ionic luminescent material sandwiched between two metal electrodes [1–5]. LECs have simple device architecture, containing ionic species which can be easily fabricated from solution process. The presence of mobile ions makes LECs insensitive to the work function of electrodes and thus providing a method to use inert metals such as Al, Au or Ag as cathodes for the fabrication [5,6]. Moreover, LECs do not require electron–hole injection layer materials and hence could be fabricated without any rigorous encapsulation process. However, multi-layered organic light-emitting diodes (OLEDs) which are composed of neutral molecules in the active layer require multi evaporation process which makes its fabrication very expensive compared to LECs. All these characteristics together with low production cost make LECs a superior candidate for the next-generation display and lighting purposes.

Ionic transition metal complexes (iTMCs) and conjugated polymers are the most widely used electroluminescent materials for the fabrication of LEC devices. Based on conjugated luminescent polymer containing an ion conducting polymer and an inorganic salt, Heeger proposed LECs in 1995 for the first time [1]. Soon after, an alternative approach was introduced by Lee et al. in 1996, in which ionic ruthenium complex was employed as the light emitting material [2]. Thereafter, iTMCs have attracted the attention of researchers due to their excellent electroluminescent properties and phosphorescent nature. The intrinsic ionic nature of iTMCs enables solubility in most of the organic polar solvents and avoids the requirement of an ion conducting material in LEC devices. Being ionic, LECs based on iTMC can perform all the necessary roles

* Corresponding author. Tel.: +82 51 510 2396; fax: +82 51 512 8634.
E-mail address: choe@pusan.ac.kr (Y. Choe).

1566-1199/$ - see front matter © 2013 Elsevier B.V. All rights reserved.
http://dx.doi.org/10.1016/j.orgel.2013.12.026

of electroluminescence such as charge injection, transport of charge carriers and emissive recombination. Moreover, iTMCs can be synthesized with relative ease and exhibits high thermal and photochemical stabilities.

The iTMCs most widely used for the fabrication of LECs are based on iridium(III) and ruthenium(II) complexes with hexafluorophosphate counter anion. LECs based on ionic Cu(I) [7–10], the cheap and non-toxic material and Os(II) [11,12] complexes were also reported in the early stages. However, the low ligand-field splitting energies (LFSEs) of Cu(I), Os(II) and Ru(II) [2,3,11,13–18], complexes makes it impractical to tune the emission color to shorter wavelength region of the visible spectrum and hence are not good candidates for LEC applications. Moreover, these complexes exhibited low luminescent efficiencies which again limit their incorporation in lighting devices [5]. In contrast, the larger LFSEs of iridium(III) makes it a superior candidate over other iTMCs and are thus capable of tuning the emission color throughout the visible region through the structural modification of organic ligands [19–29]. The first LEC based on cationic iridium complex was reported by Slinker et al. in 2004, which gave yellow light under 3 V [4]. Due to the possession of the large LFSE values along with good photo stability, LECs based on iridium complexes exhibits high efficiency and tunable emission colors and hence received great attention as a light emitting material since it was proposed [30,31].

The operation mechanism of LECs arises from the mobile ions which reduce the injection barrier for holes and electrons as proposed by two operation models such as the electrodynamic (ED) model and the electrochemical doping (ECD) model. ED model states that the mobile ions in the active layer move towards the respective electrodes under the application of an external bias and accumulate at the electrode surfaces creating an electrical double layer. This results in the generation of large electric field at the electrode surfaces, which facilitates the injection of charge carriers that undergo transport and their recombination results in the emission of light at low operating voltage.

A large number of iridium complexes were fabricated with yellow [32–34], orange [31,35–37], and red [38–40] light emission and achieved high luminance efficiencies. However, the generation of blue and green light with high efficiency and good color purity are very important for lighting purposes but the reports on these colors are scarce. This is because; the simple mixing of these primary colors would eventually lead to the development of white light, which is very essential towards the practical solid state lighting applications. There are two approaches to enlarge the energy gap of complex through the structural modification of organic ligands and hence tune the emission color to blue region. The chemical modification is achieved by introducing electron withdrawing groups to the cyclometalated ligand which decreases the highest occupied molecular orbital, HOMO energy (stabilization), whereas the tailoring of electron donating substituents on the ancillary ligands increases the energy of the lowest unoccupied molecular orbital, LUMO and results the so called destabilization of LUMO.

Herein, we report two new cationic iridium complexes, $[Ir(ppy)_2(EP\text{-}Imid)]PF_6$ (Complex 1) and $[Ir(dfppy)_2(EP\text{-}Imid)]PF_6$ (Complex 2) employing 2-(4-ethyl-2-pyridyl)-1H-imidazole (EP-Imid) as the ancillary ligand, 2-phenylpyiridine (ppy) and 2-(2,4-difluorophenyl)pyridine (dfppy) as the cyclometalated ligands. LECs were fabricated by incorporating these complexes which emits green (522 nm) and blue–green (500 nm) electroluminescence for Complexes 1 and 2 respectively. Our work suggests that imidazole based ancillary ligands are capable to destabilize the LUMOs of the heteroleptic iridium complexes and hence shifted the emission spectra to blue region and achieved current efficiency of 1.0 and 0.88 cd A^{-1} for Complexes 1 and 2 respectively.

2. Experimental

2.1. Materials and methods

Iridium(III) chloride hydrate, 99.9% ($IrCl_3{\cdot}xH_2O$) was purchased from Alfa Aesar and used without further purification. All other starting materials and solvents were purchased from Aldrich and used as received. ^1H and ^{13}C NMR spectra were recorded on a Varian Unity Inova 500 MHz FT-NMR spectrometer. Chemical shifts δ (in ppm) were measured relative to residual CD_2Cl_2 solvent with tetramethylsilane as internal standard. Elemental analyses were performed on Elementar Vario EL CHN elemental analyzer. UV–visible absorption spectra were carried out in a 1 cm path length quartz cell using Agilent 8453 spectrophotometer. Photoluminescence (PL) emission spectra of complexes in acetonitrile solutions and thin films were recorded using an F-7000 FL spectrophotometer at the excitation wavelength of 430 nm and 410 nm for Complexes 1 and 2, respectively. The surface morphology of the films was investigated using atomic force microscopy (AFM). Electrochemical measurements of the complexes (10^{-3} M) were employed in a potentiostat/galvanostat (Iviumstat) voltametric analyzer with a scan rate 100 mV s^{-1}. The electrolytic cell consists of platinum as the working electrode, platinum wire as the counter electrode and an Ag/AgCl as the reference electrode. The supporting electrolyte was 0.1 M tetrabutylammonium hexafluorophosphate ($TBAPF_6$) in CH_3CN solutions. The redox potentials of each measurement was recorded against ferrocenium/ferrocene (Fc^+/Fc) couple and used as an internal standard. The HOMO/LUMO energy levels and hence the energy gap of the complexes were calculated using the empirical relations [41,42], $E_{HOMO} = [-e(E_{ox(vs.Ag/AgCl)} - E_{1/2(Fc/Fc^+vs.Ag/AgCl)})] - 4.8$ eV; $E_{LUMO} = [-e(E_{red} - E_{1/2})] - 4.8$ eV and $E_{gap} = -E_{HOMO} - E_{LUMO}$ where E_{HOMO} is the energy level of the highest occupied molecular orbital, E_{LUMO} is the energy level of the lowest unoccupied molecular orbital, E_{gap} is the energy gap, E_{ox} is the oxidation potential, E_{red} is the reduction potential of the complex and $E_{1/2(Fc/Fc^+vs.Ag/AgCl)}$ is the reduction potential of ferrocene which was found to be 0.43 V.

2.2. Synthesis of cationic iridium complexes

Heteroleptic iridium complexes $[Ir(ppy)_2(EP\text{-}Imid)]PF_6$ (Complex 1) and $[Ir(dfppy)_2(EP\text{-}Imid)]PF_6$ (Complex 2) were synthesized by the reaction of corresponding chloro-bridged dimer with 2-(4-ethyl-2-pyridyl)-1H-imidazole

(EP-Imid) ancillary ligand according to the previously reported procedures [40,43]. The synthetic routes with structures of cationic iridium complexes are shown in Scheme 1. Cyclometalated iridium(III) chloro-bridged dimers, generally having the formula, $[Ir(C\hat{}N)_2(\mu\text{-}Cl)]_2$ were synthesized by refluxing $IrCl_3{\cdot}xH_2O$ with 2.5 equivalents of cyclometalated ligands such as 2-phenylpyridine (ppy) and 2-(2,4-difluorophenyl)pyridine (dfppy) in a mixture of 2-ethoxyethanol and water (3:1 v/v) for 24 h [44]. These dimeric iridium (III) intermediates underwent facile reaction with imidazole based ancillary ligand followed by ion exchange reaction from Cl^- to PF_6^- to yield luminescent iridium complexes in high yields. The obtained complexes were characterized by various spectroscopic, photophysical and electrochemical methods.

2.2.1. Synthesis of $[Ir(ppy)_2(EP\text{-}Imid)]PF_6$ (Complex 1)

The dichloro-bridged dimeric iridium complex $[Ir(ppy)_2Cl]_2$ (108 mg, 0.1 mmol) and Ep-Imid (38 mg, 0.22 mmol) were dissolved in a mixture of CH_2Cl_2 (15 ml) and MeOH (15 ml) and refluxed at 60 °C under nitrogen for 16 h. The reaction mixture was then cooled to room temperature and solid ammonium hexafluorophosphate (65 mg, 0.4 mmol) was added into it, stirred for 1 h at room temperature. The solvent was removed under reduced pressure. The crude product obtained was dissolved in dichloromethane and filtered to remove the inorganic impurities. The addition of hexane to the filtrate yielded the desired product as a yellow solid which was filtered off and dried at vacuum oven for 24 h. The crude material obtained was purified by column chromatography (Merck Alox 90; CH_2Cl_2 changing to CH_2Cl_2/MeOH, 100:2) yielding the desired product as yellow solid (148 mg, 0.18 mmol, 90%). ^1H NMR (500 MHz, CD_2Cl_2) δ (ppm): 11.49 (s, NH), 8.63 (d, J = 5.5 Hz, 1H), 8.53 (d, 6.3 Hz, 2H), 8.14 (d, J = 0.93 Hz, 2H), 7.93–7.91 (m, 2H), 7.78–7.68 (m, 6H), 7.60 (s, 1H), 7.56–7.54 (m, 2H), 7.33 (dd, J = 2.50 Hz and 1.43 Hz, 1H), 7.05–6.97 (m, 2H), 6.93–6.85 (m, 2H), 2.83 (q, J = 7.59 Hz, 7.59 Hz and 7.58 Hz, 2H), 1.31 (t, J = 7.59 Hz and 7.59 Hz, 3H). ^{13}C NMR (126 MHz, CD_2Cl_2) δ (ppm): 168.6, 158.5, 151.9, 150.6, 149.6, 144.9, 138.3, 132.5, 130.9, 130.5, 128.4, 126.8, 125.3, 124.9, 123.6, 122.8, 122.4, 119.9, 29.0, 13.9. Anal. Found (%): C 46.99, H 3.39, N 8.43. Anal. Calcd for $C_{32}H_{27}N_5PF_6Ir$: C 46.94, H 3.32, N 8.55.

2.2.2. Synthesis of $[Ir(dfppy)_2(EP\text{-}Imid)]PF_6$ (Complex 2)

The Complex 2, *$[Ir(dfppy)_2(EP\text{-}Imid)]PF_6$* was synthesized according to the above procedure in which the dichloro-bridged diiridium complex $[Ir(ppy)_2Cl]$ was replaced by $[Ir(dfppy)_2Cl]_2$ (122 mg, 0.1 mmol) and refluxed with Ep-Imid (38 mg, 0.22 mmol) in a mixture of CH_2Cl_2 (15 ml) and MeOH (15 ml) under nitrogen for 16 h followed by ion exchange from Cl^- to PF_6^-(142 mg, 0.15 mmol, 79%). ^1H NMR (500 MHz, CD_2Cl_2) δ (ppm): 11.49 (s, NH), 8.60 (d, J = 5.20 Hz, 1H), 8.31 (d, J = 8.2 Hz, 2H), 8.19 (s, 1H), 7.84–7.80 (m, 2H), 7.72 (d, J = 5.7 Hz, 2H), 7.67–7.65 (m, 2H), 7.53–7.50 (m, 1H), 7.09–7.02 (m, 4H), 6.68 (s, 2H), 2.86 (q, J = 7.59 Hz, 7.59 Hz and 7.57 Hz, 2H), 1.31 (t, J = 7.59 Hz and 7.59 Hz, 3H). ^{13}C NMR (126 MHz, CD_2Cl_2) δ (ppm): 165.5, 163.4, 161.2, 160.7, 159.2, 156.2, 151.7, 150.3, 149.6, 139.3, 139.2, 128.7, 128.1, 126.8, 124.1, 123.9, 123.8, 122.9, 114.8, 99.2, 29.0, 13.9. Anal. Found (%): C 43.19, H 2.66, N 7.94. Anal. Calcd for $C_{32}H_{23}N_5PF_{10}Ir$: C 43.15, H 2.60, N 7.86.

2.3. Fabrication and characterization of LEC devices

The buffer layer, poly(3,4-ethylenedioxythiophene):polystyrenesulfonate (PEDOT:PSS) was purchased from H.C. Starck. Indium tin oxide (ITO) as anode was sputtered using conventional photolithography. Prior to the deposition of organic layers, ITO substrates were cleaned by sonication in a mixture of ethanol, acetone, and isopropyl alcohol at 1:1:1 volume ratio for 30 min and finally exposed to UV-ozone for 20 min.

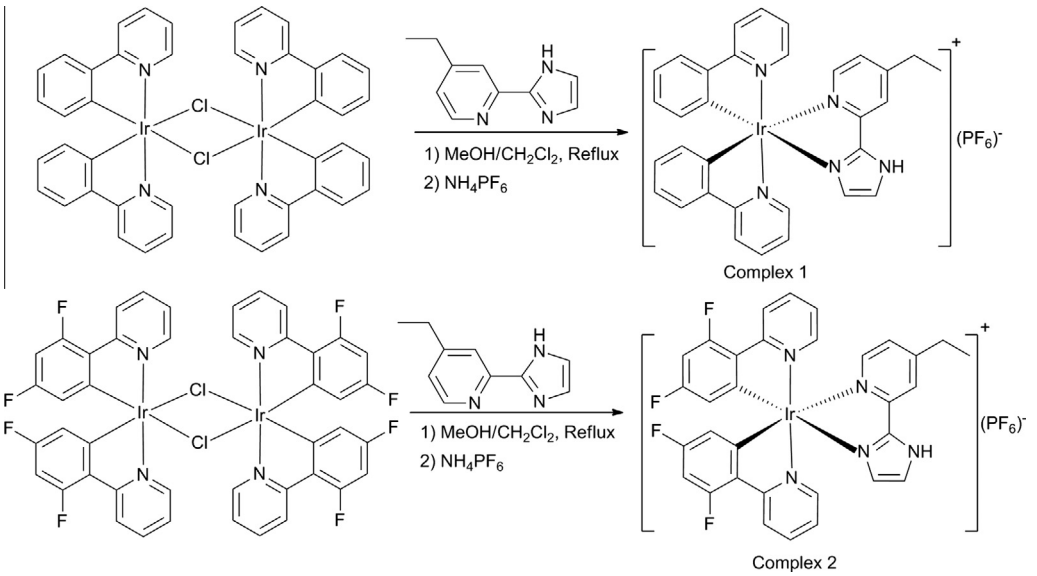

Scheme 1. The synthetic routes and structures of the cationic iridium complexes.

LECs were fabricated as follows. A thin film of PEDOT:PSS (40 nm) was spin coated onto the pre-cleaned ITO substrate at a rate of 2000 rpm for 20 s and then baked at 120 °C for 10 min. The active layer was prepared by dissolving 20 mg of the complexes in acetonitrile solutions with the concentrations of 0.024 M and 0.022 M for Complexes 1 and 2, respectively. The solutions were kept inside the shaking incubator for 24 h and then filtered using 0.1 μm PTFE-filter which were spin coated on the top of ITO/PEDOT:PSS layer at 2000 rpm for 20 s. The buffer layer, PEDOT:PSS is not only a hole injecting material but it also helps to smoothen the surface of ITO anode [39]. After spin coating the active layer (75 nm), the substrate was transferred to a hot plate at 70 °C for 1 h under vacuum. Finally, a thin film of aluminum cathode (100 nm) was deposited on the top of active layer by the thermal evaporation method using a shadow mask under high vacuum. The electroluminescent properties of the resultant devices were performed using Keithley characterization systems. The current density and luminance vs. voltage sweeps were measured using a Keithley 2400 source meter and calibrated with a silicon photodiode. An Avantes luminance spectrometer was used to measure the EL spectrum and CIE coordinates.

3. Results and discussion

3.1. Photophysical properties

The absorption spectra of the complexes in acetonitrile solutions at room temperature are shown in Fig. 1. The UV–visible absorption spectra of the complexes displays broad and an intense absorption band in the UV region ranging from 230 to 320 nm assigned to the spin-allowed ligand-centered (LC) $^1\pi$–π^* transitions in both cyclometalated and ancillary ligands. Along with these high intense LC bands, less intense absorption bands are observed from 320 nm to 400 nm which correspond to excitations to spin-allowed metal-to-ligand charge-transfer (^{1}MLCT), spin-forbidden metal-to-ligand charge-transfer (^{3}MLCT), ligand-to-ligand charge-transfer (^{3}LLCT and ^{1}LLCT) and ligand-centered (LC) $^3\pi$–π^* transitions of the complexes [45]. In addition, very weaker bands are observed at 438 nm (Complex 1) and 424 nm (Complex 2) which extends to the visible region. The blue shift in absorption spectrum of Complex 2 (424 nm) is due to the presence of electron withdrawing fluorine atoms on the cyclometalated ligand.

As shown in Fig. 2, the room temperature photoluminescence (PL) emission spectrum of the Complex 1 show vibronically structured peaks with emission maxima at 488 nm and a shoulder at 511 nm which corresponds to the light emission in the blue–green region. However, the emission spectrum of Complex 2 emits blue light with an emission peak and a shoulder at 460 and 485 nm, respectively. Compared to Complex 1, the emission spectrum of Complex 2 is blue shifted by 28 nm due to the stabilization of HOMO energy endowed by the electron withdrawing fluorine atoms. These structured emission peaks of Complexes 1 and 2 indicates that the emissive excited states have LC $^3\pi$–π^* character rather than ^{3}MLCT or ^{3}LLCT characters [39,46]. The PL emission spectra of Complexes 1 and 2 are largely blue shifted compared to other reported ionic iridium complexes containing 4,4′-di-tert-butyl-2,2′-dipyridyl (dtb-bpy) ancillary ligand such as $[Ir(ppy)_2(dtb\text{-}bpy)]PF_6$ (581 nm) [4] and $[Ir(dfppy)_2(dtb\text{-}bpy)]PF_6$ (512 nm) [47] respectively. The results demonstrates that imidazole based ancillary ligands destabilizes the LUMO orbitals largely and proves as a better candidate to tune emission color of cationic iridium complexes to blue region. In comparison with the PL spectra in solutions, the emission spectra of Complexes 1 and 2 in neat films (Fig. 2) shows broad and featureless bands with emission maxima centered at 525 and 505 nm for Complexes 1 and 2, respectively. The emission spectra of both complexes are largely red shifted in film, which indicates the strong intermolecular interactions in thin solid films. The detailed photophysical characteristics of these complexes are summarized in Table 1.

3.2. Electrochemical properties

The electrochemical properties of iridium complexes in acetonitrile solution containing 0.1 M $TBAPF_6$ was studied by cyclic voltammetry and the redox potentials are summarized in Table 1. The energy gaps of the complexes were measured from their oxidation and reduction potentials.

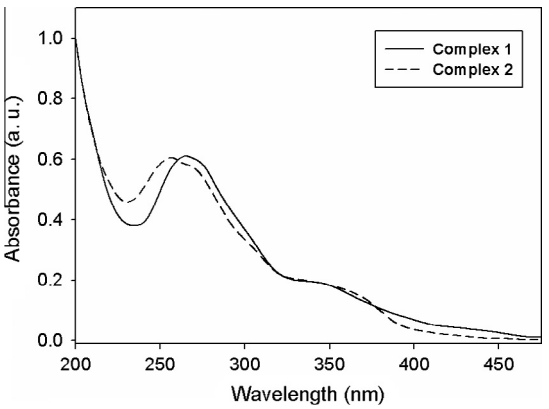

Fig. 1. UV–visible absorption spectra of cationic iridium complexes in acetonitrile solutions at room temperature.

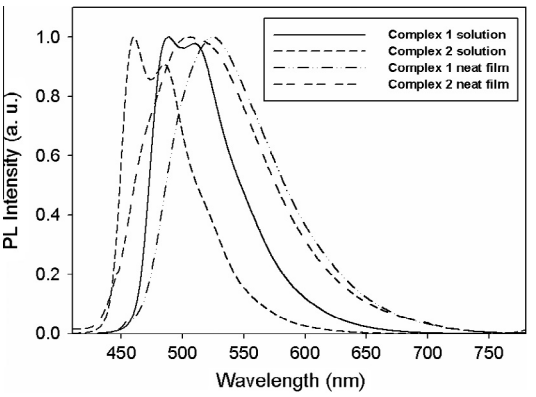

Fig. 2. Photoluminescence (PL) emission spectra of cationic iridium complexes in acetonitrile solutions and neat films at room temperature.

Table 1
Photophysical and electrochemical properties of cationic iridium complexes.

Complex	Absorbance λ_{max} (nm)	Emission at room temperature		Electrochemical data		
		Solution λ_{max} (nm)	Thin film λ_{max} (nm)	E_{ox} (V)	E_{red} (V)	Energy gap (eV)
1	266, 349, 438	488, 511	525	0.98	−2.07 −1.15	3.05
2	257, 270, 360, 424	460, 485	505	1.18	−2.03 −1.07	3.21

Fig. 3 depicts the cyclic voltammograms of the complexes which shows an irreversible oxidation peaks at 0.98 and 1.18 V for Complexes 1 and 2 respectively, and are attributed to the oxidation of Ir(III) to Ir(IV). Compared to Complex 1, the oxidation potential of Complex 2 is shifted anodically by 200 mV, assignable to the presence of electron withdrawing fluorine atoms which decrease the electron density around the iridium center and causes more difficulty to oxidize [48,49]. The complexes show reversible reduction peaks at −2.07 V for Complex 1 and −2.03 V for Complex 2 which resulted from the reduction of ancillary ligand. In addition, peaks observed at −1.15 and −1.07 V for Complexes 1 and 2 respectively are assigned to the reduction of cyclometalated ligands. The slightly lower reduction potential of Complex 2 (−1.07 V) arising from the electron withdrawing fluorine atoms on the cyclometalated ligands makes the complex more electrophilic [50]. The HOMO and the LUMO energies of the complexes were calculated from the corresponding oxidation (E_{ox}) and reduction (E_{red}) potentials and measured the HOMO–LUMO gap. The metal based HOMO stabilization and ligand based LUMO destabilization resulted in a high energy gap of 3.05 and 3.21 eV for Complexes 1 and 2 respectively, which suggest that imidazole based ancillary ligands offers a better alternative for blue shifted emissions.

3.3. DFT calculations

Density functional theory (DFT) calculations were performed in order to investigate the nature of excited states and to determine the HOMO–LUMO energy gaps thereby rationalizing the photophysical and electrochemical behaviors of the cationic iridium complexes using Gaussian 09 suite of programs. The geometries of the complexes were optimized by using B3LYP functional and the Ir atom was treated by the LANL2DZ basis set while all the other atoms were treated by 6-31G(d,p) basis set. The energy and electron density contours calculated for the HOMO and the LUMO of both complexes in the ground state are displayed in Fig. 4. The electron density distribution of the HOMO of both complexes resides on the t_{2g} orbitals of iridium ion and phenyl π orbitals of cyclometalated ligands with energies of −7.48 and −7.94 eV for Complexes 1 and 2 respectively. The lowering in HOMO energy (stabilization) of Complex 2 is arising from the electron withdrawing fluorine atoms on the cyclometalated ligands. However, the electron density contribution of the LUMO of both complexes lies on the π* orbital of ancillary ligand with an energies of –5.05 and –5.27 eV for Complexes 1 and 2 respectively. The LUMO+2 energies were calculated for both complexes which are slightly above the LUMO+1 orbitals and shows similar electron density distribution with the LUMO of both complexes. However, the LUMO+1 orbitals of Complex 2

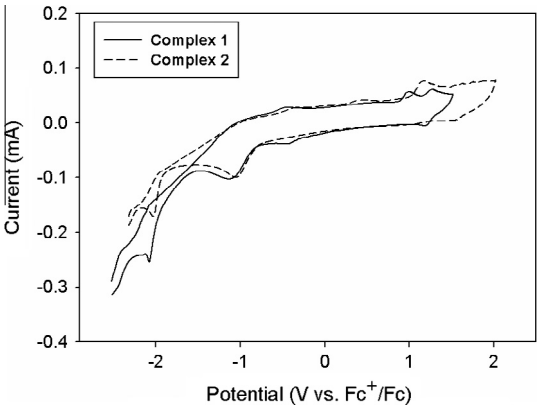

Fig. 3. Cyclic voltammograms of the complexes in acetonitrile solution (10^{-3} M). The potentials were recorded vs. Fc^+/Fc (ferrocene).

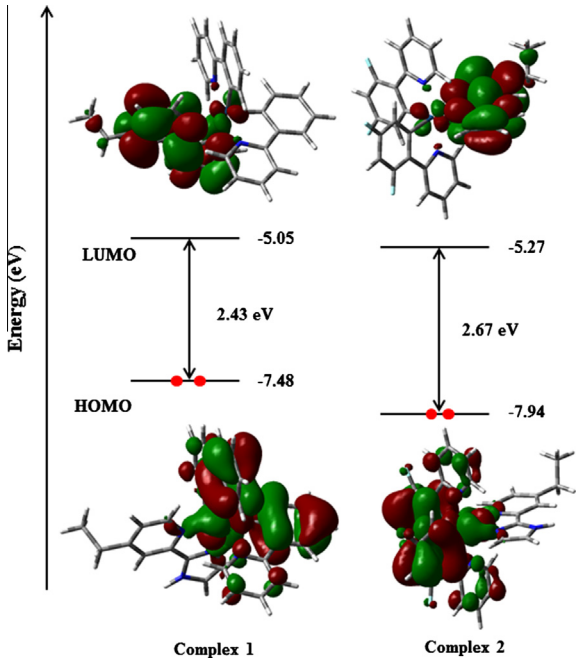

Fig. 4. The energy and electron density contours calculated for the HOMO and the LUMO of Complexes 1 and 2 in the ground state.

resides on the cyclometalated ligands unlike Complex 1, which is located on the imidazole based ancillary ligand. From the HOMO and LUMO energy values, the energy gap of 2.43 and 2.67 eV are obtained for Complexes 1 and 2 respectively which justifies the blue shift in emission spectra of Complex 2 compared to Complex 1. However, some discrepancy in energy gap is observed in theoretical and experimental values and such results have been reported for some other cationic iridium complexes [49,51].

3.4. Electroluminescent properties of LECs

To investigate the electroluminescent properties of the complexes, LECs were fabricated with the device structure of ITO/PEDOT:PSS (40 nm)/iTMC (75 nm)/Al. The surface morphology of the thin films of cationic iridium complexes spin coated on the top of PEDOT:PSS/ITO layer was studied by atomic force microscopy (AFM). The AFM images as shown in Fig. 5 show smooth surface with root–mean–square (rms) roughness of 1.39 and 3.60 nm for Complexes 1 and 2 respectively.

The electroluminescence (EL) spectra of LECs incorporating cationic iridium complexes are shown in Fig. 6. The EL spectra for both devices show broad and unstructured band which do not show any similarity with the PL spectra of corresponding iridium complexes in acetonitrile solutions indicating different emission mechanisms in both solution and solid film. LECs based on these complexes exhibit EL emission peaks at 522 nm and 500 nm for the device based on Complexes 1 and 2 respectively, which resembles the PL emission spectra of the complexes in neat film. Compared to the PL spectra in acetonitrile solution, a red shift in emission peaks was observed in the EL spectra that can be attributed to the increased intermolecular interactions between the complex molecules in thin films as seen in PL emission spectra of complexes in neat solid films [45]. LECs based on Complex 1 gave green electroluminescence with the CIE coordinates of (0.33, 0.56) and that of Complex 2 resulted in a blue–green light emission with the CIE coordinates of (0.24, 0.44). The device based on Complex 2 is blue shifted compared to that of Complex 1 by 22 nm resulting from the electron withdrawing fluorine substituents on the cyclometalated ligand which causes the stabilization of HOMO.

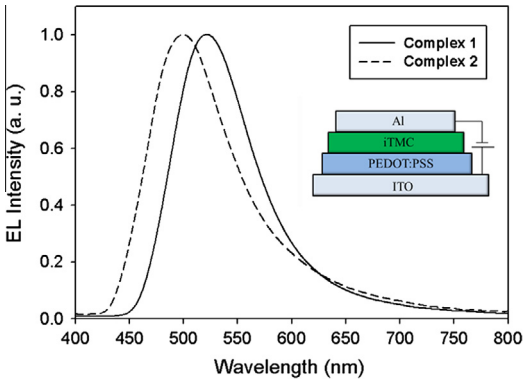

Fig. 6. Electroluminescence (EL) spectra of LECs based on cationic iridium complexes. The inset shows the device structure of LECs.

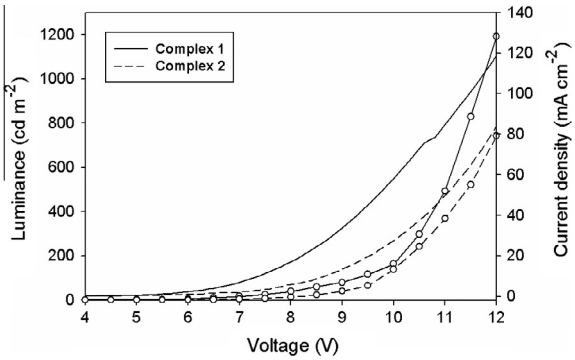

Fig. 7. Luminance and current density vs. voltage curves of LECs based on cationic iridium complexes. The lines with circle (symbol) shows luminance and the lines without any symbol shows current density of the devices.

The voltage dependent current density and voltage curves of LECs are shown in Fig. 7 and the device performances are summarized in Table 2. Fig. 7 displays that the luminance and the current density of the devices increases slowly with increase in voltage, which are typical characteristics of LEC devices [1,4]. The sluggish nature of LECs at the early stage of bias arises from the slow migration of counter ions towards the electrode surfaces that result in decreased charge carrier injection and their combinations. The

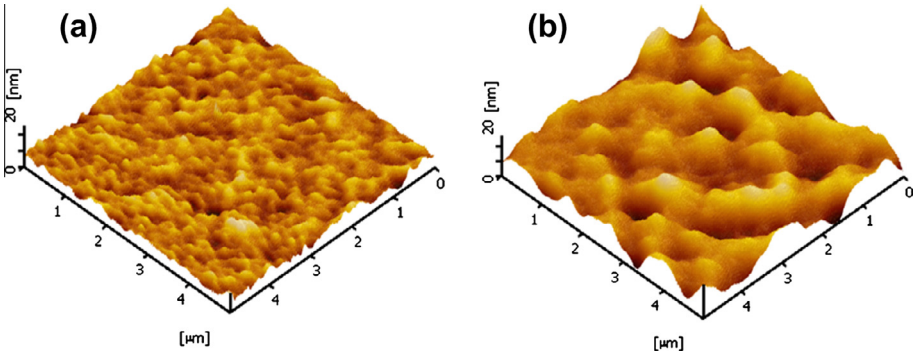

Fig. 5. AFM images of thin films on the top of PEDOT:PSS layer; (a) Complex 1 and (b) Complex 2.

Table 2
The detailed electrical characteristics of LECs based on cationic iridium complexes.

Complex	Luminance$_{max}$ (cd m^{-2})	Current density$_{max}$ (mA cm^{-2})	Current efficiency (cd A^{-1})	EL$_{max}$ (nm)	CIE coordinates
1	1191	118.78	1.0	522	(0.33, 0.56)
2	741	84.12	0.88	500	(0.24, 0.44)

luminance of the devices based on Complexes 1 and 2 increases sharply beyond 8 V with increase in voltage due to enhanced injection and recombination of both holes and electrons. It is noted that both complexes are electrically stable and kept increasing the luminance throughout the voltage scan without deteriorating its stability even at high voltage of 12 V. LECs based on Complex 1 resulted in a high luminance of 1191 cd m^{-2}, current density of 118.78 mA cm^{-2} and a peak current efficiency of 1.0 cd A^{-1}. The device fabricated using Complex 2 exhibited a maximum luminance, current density and peak current efficiency of 741 cd m^{-2}, 84.12 mA cm^{-2} and 0.88 cd A^{-1} respectively. The lower luminance and current efficiencies of LECs based on Complex 2 are resulted from the higher carrier injection barrier and unbalanced charge recombination due to their enlarged energy gap [45].

4. Conclusions

Two new blue and blue–green light-emitting cationic iridium complexes, [Ir(ppy)$_2$(EP-Imid)]PF$_6$ (Complex 1) and [Ir(dfppy)$_2$(EP-Imid)]PF$_6$ (Complex 2) with 2-(4-ethyl-2-pyridyl)-1H-imidazole as the ancillary ligand were synthesized and characterized. LECs were fabricated based on these complexes which gave green electroluminescence (522 nm) for Complex 1 with a CIE coordinates of (0.33, 0.56) and achieved a current efficiency of 1.0 cd A^{-1}. LECs based on Complex 2 gave blue–green electroluminescence (500 nm) with a CIE coordinates of (0.24, 0.44) and a current efficiency of 0.88 cd A^{-1}. Our work suggests that imidazole based ancillary ligands are better candidates to tune the emission color of LECs to blue–green region through the significant destabilization of LUMO orbitals.

Acknowledgements

This work was supported by the Basic Science Research Program through the National Research Foundation of Korea (NRF) funded by the Ministry of Education, Science and Technology (NRF-2013R1A1A4A03009795) and the Brain Korea (BK) 21 Plus Centre for Advanced Chemical Technology (21A20131800002), Republic of Korea.

References

[1] Q. Pei, G. Yu, C. Zhang, Y. Yang, A.J. Heeger, Science 269 (1995) 1086–1088.
[2] J.K. Lee, D.S. Yoo, E.S. Handy, M.F. Rubner, Appl. Phys. Lett. 69 (1996) 1686–1688.
[3] J. Slinker, D. Bernards, P.L. Houston, H.D. Abruna, S. Bernhard, G.G. Malliaras, Chem. Commun. 19 (2003) 2392–2399.
[4] J.D. Slinker, A.A. Gorodetsky, M.S. Lowry, J.J. Wang, S. Parker, R. Rohl, S. Bernhard, G.G. Malliaras, J. Am. Chem. Soc. 126 (2004) 2763–2767.
[5] J.D. Slinker, J. Rivnay, J.S. Moskowitz, J.B. Parker, S. Bernhard, H.D. Abruna, G.G. Malliaras, J. Mater. Chem. 17 (2007) 2976–2988.
[6] J.C. deMello, N. Tessler, S.C. Graham, R.H. Friend, Phys. Rev. B 57 (1998) 12951–12963.
[7] N. Armaroli, G. Accorsi, M. Holler, O. Moudam, J.F. Nierengarten, Z. Zhou, R.T. Wegh, R. Welter, Adv. Mater. 18 (2006) 1313–1316.
[8] Q.S. Zhang, Q.G. Zhou, Y.X. Cheng, L.X. Wang, D.G. Ma, X.B. Jing, F.S. Wang, Adv. Funct. Mater. 16 (2006) 1203–1208.
[9] V. Kalsani, M. Schmittel, A. Listorti, G. Accorsi, N. Armaroli, Inorg. Chem. 45 (2006) 2061–2067.
[10] M. Felici, P. Contreras-Carballada, J.M.M. Smits, R.J.M. Nolte, R.M. Williams, L. De Cola, M.C. Feiters, Molecules 15 (2010) 2039–2059.
[11] F.G. Gao, A.J. Bard, Chem. Mater. 14 (2002) 3465–3470.
[12] A.R. Hosseini, C.Y. Koh, J.D. Slinker, S.F. Torres, H.D. Abruna, G.G. Malliaras, Chem. Mater. 17 (2005) 6114–6116.
[13] H.J. Bolink, L. Cappelli, E. Coronado, P. Gavina, Inorg. Chem. 44 (2005) 5966–5968.
[14] G. Kalyuzhny, M. Buda, J. McNeill, P. Barbara, A.J. Bard, J. Am. Chem. Soc. 125 (2003) 6272–6283.
[15] C.H. Lyons, E.D. Abbas, J.K. Lee, M.F. Rubner, J. Am. Chem. Soc. 120 (1998) 12100–12107.
[16] L.J. Soltzberg, J.D. Slinker, S. Flores-Torres, D.A. Bernards, G.G. Malliaras, H.D. Abruña, J.S. Kim, R.H. Friend, M.D. Kaplan, V. Goldberg, J. Am. Chem. Soc. 128 (2006) 7761–7764.
[17] H. Rudmann, M.F. Rubner, J. Appl. Phys. 90 (2001) 4338–4345.
[18] F.G. Gao, A.J. Bard, J. Am. Chem. Soc. 122 (2000) 7426–7427.
[19] R.D. Costa, E. Ortí, H.J. Bolink, S. Graber, C.E. Housecroft, E.C. Constable, Chem. Commun. 47 (2011) 3207–3209.
[20] R.D. Costa, E. Ortí, D. Tordera, A. Pertegás, H.J. Bolink, S. Graber, C.E. Housecroft, L. Sachno, M. Neuburger, E.C. Constable, Adv. Energy Mater. 1 (2011) 282–290.
[21] L. He, L. Duan, J. Qiao, D. Zhang, L. Wang, Y. Qiu, Chem. Commun. 47 (2011) 6467–6469.
[22] B. Chen, Y. Li, W. Yang, W. Luo, H. Wu, Org. Electron. 12 (2011) 766–773.
[23] L. Sun, A. Galan, S. Ladouceur, J.D. Slinker, E.Z. Colman, J. Mater. Chem. 21 (2011) 18083–18088.
[24] H.B. Wu, H.F. Chen, C.T. Liao, H.C. Su, K.T. Wong, Org. Electron. 13 (2012) 483–490.
[25] F. Kessler, R.D. Costa, D.D. Censo, R. Scopelliti, E. Ortí, H.J. Bolink, S. Meier, W. Sarfert, M. Grätzel, M.K. Nazeeruddin, E. Baranoff, Dalton Trans. 41 (2012) 180–191.
[26] C.D. Sunesh, O. Sunseong, M. Chandran, D. Moon, Y. Choe, Mater. Chem. Phys. 136 (2012) 173–178.
[27] C.D. Sunesh, G. Mathai, Y.R. Cho, Y. Choe, Polyderon 57 (2013) 77–82.
[28] D. Tordera, A. Pertegas, N.M. Shavaleev, R. Scopelliti, E. Ortí, H.J. Bolink, E. Baranoff, M. Gratzel, M.K. Nazeeruddin, J. Mater. Chem. 22 (2012) 19264–19268.
[29] S.B. Meier, W. Sarfert, J.M. Junquera-Hernández, M. Delgado, D. Tordera, E. Ortí, H.J. Bolink, F. Kessler, R. Scopelliti, M. Grätzel, M.K. Nazeeruddind, E. Baranoff, J. Mater. Chem. C 1 (2013) 58–68.
[30] B. Chen, Y. Li, Y. Chu, A. Zheng, J. Feng, Z. Liu, H. Wu, W. Yang, Org. Electron. 14 (2013) 744–753.
[31] H. Su, F.C. Fang, T.Y. Hwu, H.H. Hsieh, H.F. Chen, G.H. Lee, S.M. Peng, K.T. Wong, C.C. Wu, Adv. Funct. Mater. 17 (2007) 1019–1027.
[32] H.C. Su, Y.H. Lin, C.H. Chang, H.W. Lin, C.C. Wu, F.C. Fang, H.F. Chen, K.T. Wong, J. Mater. Chem. 20 (2010) 5521–5526.
[33] L. He, J. Qiao, L. Duan, G.F. Dong, D.Q. Zhang, L.D. Wang, Y. Qiu, Adv. Funct. Mater. 19 (2009) 2950–2960.
[34] H.C. Su, C.C. Wu, F.C. Fang, K.T. Wong, Appl. Phys. Lett. 89 (2006) 261118–261120.
[35] C.T. Liao, H.F. Chen, H.C. Su, K.T. Wong, Phys. Chem. Chem. Phys. 14 (2012) 9774–9784.
[36] R.D. Costa, E. Orti, H.J. Bolink, S. Graber, S. Schaffner, M. Neuburger, C.E. Housecroft, E.C. Constable, Adv. Funct. Mater. 19 (2009) 3456–3463.
[37] R.D. Costa, G. Fernandez, L. Sanchez, N. Martin, E. Orti, H.J. Bolink, Chem. – Eur. J. 16 (2010) 9855–9863.
[38] C.T. Liao, H.F. Chen, H.C. Su, K.T. Wong, Phys. Chem. Chem. Phys. 14 (2012) 1262–1269.

[39] A.B. Tamayo, S. Garon, T. Sajoto, P.I. Djurovich, I.M. Tsyba, R. Bau, M.E. Thompson, Inorg. Chem. 44 (2005) 8723–8732.
[40] R.D. Costa, F.J. Cespedes-Guirao, E. Orti, H.J. Bolink, J. Gierschner, F. Fernandez-Lazaro, A. Sastre-Santos, Chem. Commun. (2009) 3886–3888.
[41] Y. Liu, M.S. Liu, A.K.-Y. Jen, Acta Polym. 50 (1999) 105–108.
[42] S.W. Hwang, Y. Chen, Macromolecules 34 (2001) 2981–2986.
[43] S. Sprouse, K.A. King, P.J. Spellane, R.J. Watts, J. Am. Chem. Soc. 106 (1984) 6647–6653.
[44] M. Nonoyama, Bull. Chem. Soc. Jpn. 47 (1974) 767–768.
[45] L. He, L. Duan, J. Qiao, R. Wang, P. Wei, L. Wang, Y. Qiu, Adv. Funct. Mater. 18 (2008) 2123–2131.
[46] M.G. Colombo, H.U. Gudel, Inorg. Chem. 32 (1993) 3081–3087.
[47] H.J. Bolink, E. Coronado, R.D. Costa, N. Lardieś, E. Ortí, Inorg. Chem. 47 (2008) 9149–9151.
[48] C. Adachi, R.C. Kwong, P. Djurovich, V. Adamovich, M.A. Baldo, M.E. Thompson, S.R. Forrest, Appl. Phys. Lett. 79 (2001) 2082–2084.
[49] M.S. Lowry, J.I. Goldsmith, J.D. Slinker, R. Rohl, R.A. Pascal, G.G. Malliaras, S. Bernhard, Chem. Mater. 17 (2005) 5712–5719.
[50] J. Brooks, Y. Babayan, S. Lamansky, P.I. Djurovich, I. Tsyba, R. Bau, M.E. Thompson, Inorg. Chem. 41 (2002) 3055–3066.
[51] M.K. Nazeeruddin, R.T. Wegh, Z. Zhou, C. Klein, Q. Wang, F. De Angelis, S. Fantacci, M. Gratzel, Inorg. Chem. 45 (2006) 9245–9250.

ACS APPLIED MATERIALS & INTERFACES

Research Article

www.acsami.org

Constructive Effects of Long Alkyl Chains on the Electroluminescent Properties of Cationic Iridium Complex-Based Light-Emitting Electrochemical Cells

Chozhidakath Damodharan Sunesh,[†] George Mathai,[‡] and Youngson Choe*,[†]

[†]Department of Polymer Science and Chemical Engineering, Pusan National University, Busan 609-735, South Korea

[‡]Department of Chemistry, Sacred Heart College, Thevara, Kochi 682-013, India

ABSTRACT: A series of cationic iridium complexes (**1**–**6**) were synthesized using alkylated imidazole-based ancillary ligands, and the photophysical and electrochemical properties of these complexes were subsequently evaluated. Light-emitting electrochemical cells (LECs) were fabricated from these complexes, and the effects of the alkyl chain length on the electroluminescent properties of the devices were investigated. The LECs based on these complexes resulted in yellow emission (complexes **1**, **3**, and **5**) and green emission (complexes **2**, **4**, and **6**) with Commission Internationale de L'Eclairage (CIE) coordinates of (0.49, 0.50) and (0.33, 0.59), respectively. Our results indicate that the luminance and efficiency of the LECs can consistently be enhanced by increasing the alkyl chain length of the iridium complexes as a result of suppressed intermolecular interaction and self-quenching. Subsequently, a high luminance of 7309 cd m^{-2} and current efficiency of 3.85 cd A^{-1} were achieved for the LECs based on complex **5**.

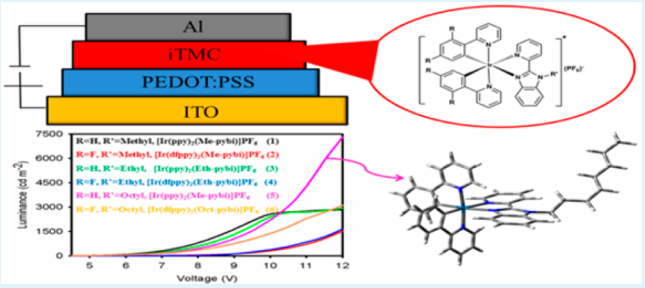

KEYWORDS: *light-emitting electrochemical cells, iridium complexes, alkyl chain length, steric hindrance, electroluminescence*

1. INTRODUCTION

Light-emitting electrochemical cells (LECs) are the next generation of optoelectronic devices and commonly employ ionic transition metal complexes (iTMCs) or conjugated polymers as the light-emitting material.[1−5] LECs typically consist of ionic species, which are fabricated in solution and utilize air-stable electrodes, allowing the nonrigorous encapsulation of the devices.[6] This simple device architecture employs ionic species that migrate toward the respective electrodes under an external bias; subsequent carrier injection and recombination results in the emission of light. These features make LECs a superior candidate for the next generation of display and lighting applications compared to sophisticated multilayered organic light-emitting diodes (OLEDs), which are composed of neutral molecules and require multiple evaporation processes that cause the fabrication of such devices to be quite expensive.

The first solid-state LEC was reported in 1995 and consisted of a polymer blend sandwiched between two electrodes.[1] The polymer blend was composed of a mixture containing an emissive conjugated polymer, an ion conducting polymer, and an inorganic salt. More recently, LECs based on iTMCs have attracted significant attention owing to their various advantages over polymer-based LECs. In general, iTMCs possess desirable thermal and photochemical stabilities. Additionally, iTMCs exhibit high luminance efficiencies owing to the phosphorescent nature of the metal complexes. They are also intrinsically ionic and contribute to both charge transport and emissive recombination processes and subsequently eliminate the need for the ion-conducting materials used in polymer-based devices. Unlike iTMCs, polymer-based LECs containing multiple components may result in aggregation or phase separation that negatively affects the thin film morphology and limits the device performance. These characteristics make iTMCs the most promising ionic emitter for the fabrication of optoelectronic devices. The first solid state LECs based on iTMCs were reported in 1996 and utilized an ionic ruthenium polypyridyl complex.[3] Extensive effort has since been carried out to enhance the device performance of LECs incorporating iTMCs.

LECs based on various iTMCs such as ionic Ru(II),[3,4,7−13] Os(II),[13,14] and Cu(I)[15−18] complexes have been previously reported. However, these complexes are unable to tune the emission colors to shorter wavelengths because of their limited ligand field splitting energies (LFSEs) and therefore have limited applications in LECs. LECs based on iridium complexes were fabricated for the first time in 2004 with the intention of producing emission wavelengths in the blue region, but they subsequently produced a yellow emission with an efficiency of 5%.[19] The larger LFSEs of Ir(III) makes it a superior material over other iTMCs, and it can produce multicolor devices through the selection of appropriate organic ligands.[20−44] The structural modification was performed by introducing electron

Received: February 25, 2014
Accepted: September 23, 2014

   dx.doi.org/10.1021/am5058426 | *ACS Appl. Mater. Interfaces* XXXX, XXX, XXX−XXX

Scheme 1. Synthetic Routes and Structures of Cationic Iridium Complexes 1−6

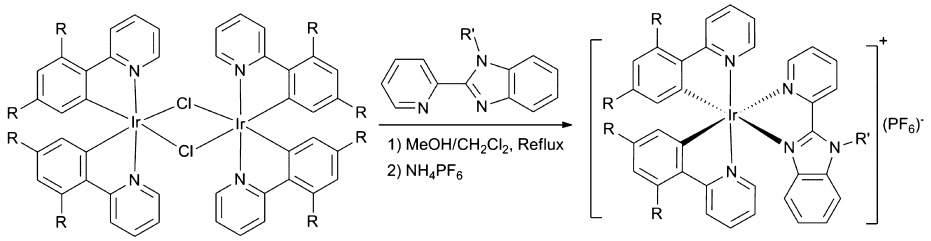

R=H, R'=Methyl, $[Ir(ppy)_2(Me\text{-}pybi)]PF_6$ (1)
R=F, R'=Methyl, $[Ir(dfppy)_2(Me\text{-}pybi)]PF_6$ (2)
R=H, R'=Ethyl, $[Ir(ppy)_2(Eth\text{-}pybi)]PF_6$ (3)
R=F, R'=Ethyl, $[Ir(dfppy)_2(Eth\text{-}pybi)]PF_6$ (4)
R=H, R'=Octyl, $[Ir(ppy)_2(Oct\text{-}pybi)]PF_6$ (5)
R=F, R'=Octyl, $[Ir(dfppy)_2(Oct\text{-}pybi)]PF_6$ (6)

withdrawing groups into the cyclometalated ligand or by attaching electron donating groups to the ancillary ligand. These methods resulted in the enlarged energy gaps through the stabilization of the highest occupied molecular orbital (HOMO) and destabilization of the lowest unoccupied molecular orbital (LUMO).

In addition to tuning the emission colors, it is also necessary to produce a device that exhibits high luminance and efficiency. Steric hindrance is the best strategy because it decreases the intermolecular interaction between the metal complexes.[34] The active layer is composed of neat films; therefore, self-quenching will occur and produce an unbalanced carrier injection/recombination that diminishes the performance of the devices. In order to suppress the intermolecular interactions and self-quenching, the complexes should be as far away from each other as possible through the selective design of organic ligands. In 2013, Zhang et al.[24] reported yellow light-emitting LECS based on cationic iridium complexes using 1,3,4-oxadiazole (OXD) derivatives as the cyclometalated and ancillary ligands. LECS based on these complexes exhibited a maximum brightness of 22.0 cd m^{-2} and a current efficiency of 0.18 cd A^{-1}. Recently, we reported two cationic iridium complexes using the imidazole-based ancillary ligand 2-(4-ethyl-2-pyridyl)-1*H*-imidazole (EP-Imid), which resulted in blue-green emission for $[Ir(ppy)_2(EP\text{-}Imid)]PF_6$ (**C1**) and green emission for $[Ir(dfppy)_2(EPImid)]PF_6$ (**C2**) (where ppy is 2-phenylpyridine and dfppy is 2-(2,4-difluorophenyl)pyridine).[33] Although color tuning was achieved using these complexes, the complexes only produced a maximum current efficiency of 1.0 cd A^{-1} and 0.88 cd A^{-1} for **C1** and **C2**, respectively, owing to the strong intermolecular interactions within the thin solid films. To reduce these interactions, as well as self-quenching, we purposefully designed ancillary ligands with various chain lengths containing methyl, ethyl, and octyl groups.

In this study, we report a series of cationic iridium complexes (**1**−**6**) using imidazole-based ancillary ligands, which were prepared by the alkylation of 2-(pyridin-2-yl)-1*H*-benzo[*d*]-imidazole (Hpybi) with various alkyl halides of varying chain lengths. The effects of the alkyl chain lengths on the electroluminescent properties of LECs were investigated. The device based on complexes **1**, **3**, and **5** produced yellow emissions, while complexes **2**, **4**, and **6** resulted in green emission colors with respect to the selection of cyclometalating ligands such as ppy or dfppy. Although the increase in alkyl chain length did not yield any significant color tuning, it resulted in enhanced luminance from the methyl to the octyl group. Consequently, a luminance of 7309 cd m^{-2} and a current efficiency of 3.85 cd A^{-1} were achieved for the LECs containing complex **5**. Our results reveal the necessity of reduced intermolecular interactions in cationic iridium complexes for the fabrication of highly efficient LEC devices.

2. EXPERIMENTAL SECTION

2.1. Materials and Methods. All reactants and solvents were purchased from Sigma-Aldrich, South Korea, except iridium(III) chloride hydrate, 99.9% ($IrCl_3{\cdot}xH_2O$) that was purchased from Alfa Aesar and used without further purification. ^1H and ^{13}C NMR spectra were recorded on a Varian Unity Inova 500 MHz FT−NMR spectrometer, and the chemical shifts δ (in ppm) were measured relative to the residual CD_2Cl_2 solvent peak with tetramethylsilane as an internal standard. Elemental analyses were performed on Elementar Vario EL CHN elemental analyzer. Solution UV−visible (UV−vis) absorption spectra and photoluminescence (PL) emission spectra of the iridium complexes were acquired in a 1 cm path-length quartz cell using an Agilent 8453 spectrophotometer and an F−7000 FL spectrophotometer, respectively. PL quantum yields (PLQYs) were measured in acetonitrile solutions at an excitation wavelength of 420 nm with quinine sulfate (Φ_p = 0.545 in 1 M H_2SO_4) as the reference substance. Electrochemical measurements of the complexes (10^{-3} M) were performed using cyclic voltammetry and recorded using a potentiostat/galvanostat (Iviumstat) voltametric analyzer with a scan rate of 100 mVs^{-1}. The electrolytic cell contained platinum as the working electrode, platinum wire as the counter electrode, and Ag/AgCl as the reference electrode. The supporting electrolyte was a 0.1 M solution of tetrabutylammonium hexafluorophosphate ($TBAPF_6$) in acetonitrile. The redox potentials of each measurement were recorded against the ferrocenium/ferrocene (Fc^+/Fc) couple that was used as an internal standard. The HOMO/LUMO energy levels and the energy gap (E_{gap}) of the complexes were calculated from the oxidation (E_{ox}) and reduction (E_{red}) potentials using the empirical relations:[45,46] $E_{HOMO} = [-e(E_{ox\ (vs\ Ag/AgCl)} - E_{1/2\ (Fc/Fc+\ vs\ Ag/AgCl)})] - 4.8$ eV; $E_{LUMO} = [-e(E_{red} - E_{1/2})] - 4.8$ eV and $E_{gap} = E_{HOMO} - E_{LUMO}$; where $E_{1/2\ (Fc/Fc+\ vs\ Ag/AgCl)}$ is the redox potential of ferrocene, which was found to be 0.43 V. E_{HOMO} and E_{LUMO} are the energy levels of the HOMO and LUMO, respectively.

2.2. Synthesis of Ancillary Ligands. *2.2.1. 1-Methyl-2-(pyridin-2-yl)-1H-benzo[d]imidazole (Me-pybi).* Me-pybi was synthesized from the precursor 2-(pyridin-2-yl)-1*H*-benzo[*d*]imidazole (Hpybi) with a yield of 79%. A solution of 35% NaOH was added to a solution of Hpybi (1 g, 5.12 mmol) in 12 mL of DMF. The resulting mixture was stirred at room temperature for 30 min, and then iodomethane (6.14 mmol) was added dropwise with constant stirring for 12 h. The reaction mixture was subsequently extracted with water and ether to remove DMF and excess NaOH. The organic layer was isolated, dried over anhydrous Na_2SO_4, and filtered. The solvent was then removed under reduced pressure. The purification of the crude product was

dx.doi.org/10.1021/am5058426 | ACS Appl. Mater. Interfaces XXXX, XXX, XXX−XXX

carried out by column chromatography on silica gel (200−300 mesh) with hexane/ethyl acetate (9:1) as the eluent to yield brown oil that crystallized into a brown solid after a week of standing. ^{1}H NMR (500 MHz, CD_2Cl_2) δ (ppm): 8.65 (d, J = 4.64 Hz, 1H), 8.37 (d, J = 7.99 Hz, 1H), 7.88−7.84 (m, 1H), 7.77−7.75 (m, 1H), 7.47−7.45 (m, 1H), 7.37−7.28 (m, 3H), 4.27 (s, 3H).

2.2.2. 1-Ethyl-2-(pyridin-2-yl)-1H-benzo[d]imidazole (Eth-pybi). Eth-pybi was synthesized following the same procedure as Me-phybi, except that iodomethane was replaced with iodoethane. Yield: 74%. ^{1}H NMR (500 MHz, CD_2Cl_2) δ (ppm): 8.69 (d, J = 4.62 Hz, 1H), 8.43 (d, J = 8.01 Hz, 1H), 7.86−7.81 (m, 2H), 7.47−7.44 (m, 1H), 7.36−7.29 (m, 3H), 4.87 (q, J = 7.13 Hz, 7.13 and 7.12 Hz, 2H), 1.49 (t, J = 7.13 and 7.13 Hz, 3H).

2.2.3. 1-Octyl-2-(pyridin-2-yl)-1H-benzo[d]imidazole (Oct-pybi). Oct-pybi was synthesized using 1-bromooctane as the alkylating agent to yield a colorless oil after column chromatography. Yield: 80%. ^{1}H NMR (500 MHz, CD_2Cl_2) δ (ppm): 8.68 (d, J = 4.65 Hz, 1H), 8.38 (d, J = 8.02 Hz, 1H), 7.84−7.80 (m, 2H), 7.45−7.42 (m, 1H), 7.34−7.26 (m, 3H), 4.82−4.78 (m, 2H), 1.89−1.82 (m, 4H), 1.40−1.30 (m, 6H), 1.34−1.22 (m, 2H), 0.85 (t, J = 6.92 and 6.92 Hz, 3H).

2.3. Synthesis of Cationic Iridium Complexes. The dimeric Ir(III) intermediates, $[Ir(\hat{C}N)_2(\mu\text{-}Cl)]_2$, were synthesized by refluxing $IrCl_3{\cdot}xH_2O$ with 2.5 eq of specific cyclometalated ligands ($\hat{C}N$) such as 2-phenylpyridine (ppy) or 2-(2,4-difluorophenyl)pyridine (dfppy) according to previously reported procedures.[47] All cationic iridium complexes were synthesized in the same manner in which the dimeric Ir(III) intermediates underwent facile reaction with alkylated imidazole-based ancillary ligands followed by ion exchange with ammonium hexafluorophosphate (NH_4PF_6) to afford phosphorescent iridium complexes in high yields.[48] The resulting complexes were then characterized by various spectroscopic, photophysical, and electrochemical methods. The synthetic routes including the structures of the cationic iridium complexes are shown in Scheme 1. The synthesis of $[Ir(ppy)_2(Me\text{-}pybi)]PF_6$ (**1**) is described in detail, and all the other complexes were synthesized by following a similar procedure.

*2.3.1. Synthesis of $[Ir(ppy)_2(Me\text{-}pybi)]PF_6$ (**1**).* The chloro-bridged dimeric iridium complex $[Ir(ppy)_2Cl]_2$ (108 mg, 0.1 mmol) and Me-pybi (52 mg, 0.25 mmol) were dissolved in a mixture of CH_2Cl_2 (15 mL) and MeOH (15 mL) that was heated to reflux under nitrogen with constant stirring for 16 h. Upon cooling to room temperature, solid NH_4PF_6 (65 mg, 0.4 mmol) was added into the reaction mixture and stirred for 1 h. The solvent was removed under reduced pressure following the addition of dichloromethane to remove any insoluble inorganic impurities. The addition of hexane to the filtrate yielded the desired product as a yellow solid, which was then filtered and dried in a vacuum oven for 24 h. The crude material was subsequently recrystallized from an acetonitrile/hexane mixture. Yield: 141 mg, 0.17 mmol, 82%. ^{1}H NMR (500 MHz, CD_2Cl_2) δ (ppm): 8.59 (d, J = 8.20 Hz, 1H), 8.21−8.17 (m, 1H), 8.10 (d, 4.56 Hz, 1H), 7.95 (d, J = 7.87 Hz, 1H), 7.89 (d, J = 7.86 Hz, 2H), 7.78−7.67 (m, 4H), 7.61−7.58 (m, 2H), 7.52−7.42 (m, 2H), 7.13−7.03 (m, 3H), 6.99−6.91 (m, 4H), 6.43−6.33 (m, 3H), 4.43 (s, 3H). ^{13}C NMR (126 MHz, CD_2Cl_2) δ (ppm): 168.3, 152.6, 151.4, 149.9, 149.1, 147.6, 147.4, 144.7, 144.5, 139.9, 138.4, 137.2, 132.7, 131.9, 131.1, 130.4, 128.5, 126.6, 125.7, 125.0, 123.7, 122.8, 120.1, 118.7, 111.7, 33.8. Anal. calcd (%) for $C_{35}H_{27}N_5PF_6Ir$: C 49.18, H 3.18, N 8.19; found, C 49.21, H 3.15, N 8.24.

*2.3.2. Synthesis of $[Ir(dfppy)_2(Me\text{-}pybi)]PF_6$ (**2**).* Complex **2** was synthesized from $[Ir(dfppy)_2Cl]_2$ (122 mg, 0.1 mmol) and Me-pybi (52 mg, 0.25 mmol) in a mixture of CH_2Cl_2/MeOH under nitrogen followed by ion exchange from Cl^- to PF_6^-. Yield: 166 mg, 0.18 mmol, 90%. ^{1}H NMR (500 MHz, CD_2Cl_2) δ (ppm): 8.64 (d, J = 8.19 Hz, 1H), 8.32 (d, J = 8.35 Hz, 1H), 8.28−8.24 (m, 3H), 8.07 (d, J = 1.74 Hz, 1H), 7.83−7.75 (m, 2H), 7.60 (d, J = 8.46 Hz, 1H), 7.53−7.48 (m, 2H), 7.18−7.15 (m, 2H), 7.05−6.97 (m, 3H), 6.83−6.89 (m, 3H), 6.38 (d, J = 8.28 Hz, 1H), 4.45 (s, 3H). ^{13}C NMR (126 MHz, CD_2Cl_2) δ (ppm): 164.7, 163.2, 161.1, 155.1, 152.4, 151.1, 150.1, 149.3, 147.4, 140.7, 139.5, 139.4, 139.3, 137.1, 128.8, 126.9, 126.2, 124.2, 124.0, 123.8, 118.1, 114.9, 114.2, 112.1, 99.5, 33.9. Anal. calcd (%) for $C_{35}H_{23}N_5PF_{10}Ir$, C 45.36, H 2.50, N 7.56; found, C 45.41, H 2.55, N 7.65.

*2.3.3. Synthesis of $[Ir(ppy)_2(Eth\text{-}pybi)]PF_6$ (**3**).* The synthesis of **3** was similar to that of **1**, except that Me-pybi was replaced by Eth-pybi. Yield: 148 mg, 0.17 mmol, 85%. ^{1}H NMR (500 MHz, CD_2Cl_2) δ (ppm): 8.43 (d, J = 7.1 Hz, 1H), 8.25−8.22 (m, 1H), 8.12 (d, 4.3 Hz, 1H), 7.96 (d, J = 8.0 Hz, 1H), 7.90 (d, J = 7.95 Hz, 2H), 7.78−7.70 (m, 4H), 7.65−7.60 (m, 2H), 7.50−7.44 (m, 2H), 7.14−7.04 (m, 3H), 6.99−6.90 (m, 4H), 6.42−6.30 (m, 3H), 4.98 (q, J = 7.18 Hz, 7.17 and 7.17 Hz, 2H), 1.71 (t, J = 7.32 and 7.32 Hz, 3H). ^{13}C NMR (126 MHz, CD_2Cl_2) δ (ppm): 168.4, 152.6, 151.7, 149.9, 149.0, 147.4, 147.3, 144.6, 144.5, 140.0, 138.4, 137.2, 132.7, 131.9, 131.1, 130.4, 128.5, 126.6, 125.7, 125.1, 123.7, 122.8, 120.1, 118.7, 111.9, 39.8, 24.7. Anal. calcd (%) for $C_{36}H_{29}N_5PF_6Ir$, C 49.77, H 3.36, N 8.06; found, C 49.79, H 3.39, N 8.01.

*2.3.4. Synthesis of $[Ir(dfppy)_2(Eth\text{-}pybi)]PF_6$ (**4**).* Complex **4** was synthesized by reacting $[Ir(dfppy)_2Cl]_2$ and Eth-pybi. Yield: 174 mg, 0.19 mmol, 92%. ^{1}H NMR (500 MHz, CD_2Cl_2) δ (ppm): 8.63 (d, J = 4.76 Hz, 1H), 8.48 (d, J = 8.3 Hz, 1H), 8.34−8.26 (m, 3H), 8.16 (d, J = 1.74 Hz, 1H), 8.10−8.07 (m, 2H), 7.84−7.64 (m, 4H), 7.56−7.47 (m, 2H), 7.06−6.97 (m, 2H), 6.69−6.60 (m, 3H), 6.51 (d, 8.35 Hz, 1H), 4.98 (q, J = 7.22 Hz, 7.22 and 7.21 Hz, 2H), 1.71 (t, J =7.32 and 7.32 Hz, 3H). ^{13}C NMR (126 MHz, CD_2Cl_2) δ (ppm): 164.7, 163.2, 161.0, 155.1, 152.4, 151.1, 150.1, 149.3, 147.4, 140.7, 139.5, 139.4, 139.2, 137.1, 128.9, 126.9, 126.2, 124.2, 124.0, 123.8, 118.1, 114.9, 114.2, 112.1, 99.5, 39.8, 24.7. Anal. calcd (%) for $C_{36}H_{25}N_5PF_{10}Ir$, C 45.96, H 2.68, N 7.44; found, C 45.93, H 2.73, N 7.49.

*2.3.5. Synthesis of $[Ir(ppy)_2(Oct\text{-}pybi)]PF_6$ (**5**).* Complex **5** was synthesized by reacting $[Ir(ppy)_2Cl]_2$ and Oct-pybi. Yield: 162 mg, 0.17 mmol, 85%. ^{1}H NMR (500 MHz, CD_2Cl_2) δ (ppm): 8.37 (d, J = 8.23 Hz, 1H), 8.24−8.20 (m, 1H), 8.1 (d, 5.43 Hz, 1H), 7.96 (d, J = 7.92 Hz, 1H), 7.89 (d, J = 7.88 Hz, 2H), 7.78−7.69 (m, 4H), 7.64−7.62 (m, 1H), 7.59 (d, J = 8.44 Hz, 1H), 7.49−7.43 (m, 2H), 7.14−7.04 (m, 3H), 6.99−6.90 (m, 4H), 6.42−6.32 (m, 3H), 4.84−4.74 (m, 2H), 2.12−1.98 (m, 4H),1.54−1.43 (m, 6H), 1.39−1.19 (m, 2H), 0.86 (t, J = 6.88 and 6.88 Hz, 3H). ^{13}C NMR (126 MHz, CD_2Cl_2) δ (ppm): 168.3, 152.7, 151.8, 151.5, 149.7, 148.9, 147.5, 144.6, 144.4, 140.1, 138.4, 136.9, 132.6, 131.9, 131.1, 130.5, 128.5, 126.7, 125.8, 125.2, 123.7, 122.9, 120.1, 118.8, 111.9, 46.6, 32.1, 30.2, 29.5, 27.1, 22.9, 14.2. Anal. calcd (%) for $C_{42}H_{41}N_5PF_6Ir$, C 52.93, H 4.34, N 7.35; found, C 52.97, H 4.36, N 7.42.

*2.3.6. Synthesis of $[Ir(dfppy)_2(Oct\text{-}pybi)]PF_6$ (**6**).* Complex **6** was synthesized by reacting $[Ir(dfppy)_2Cl]_2$ and Oct-pybi. Yield (186 mg, 0.18 mmol, 91%). ^{1}H NMR (500 MHz, CD_2Cl_2) δ (ppm): 8.44 (d, J = 8.22 Hz, 1H), 8.24−8.20 (m, 3H), 8.11 (d, J = 5.36 Hz, 1H), 7.85−7.77 (m, 3H), 7.66−7.62 (m, 2H), 7.56−7.47 (m, 3H),7.19 (t, J = 7.79 and 7.79 Hz, 1H), 7.05−6.96 (m, 2H), 6.68−6.60 (m, 3H), 6.51 (d, 8.38 Hz, 1H), 4.87−4.76 (m, 2H), 2.09−1.98 (m, 4H),1.49−1.43 (m, 6H), 1.40−1.19 (m, 2H), 0.90 (t, J = 6.99 and 6.99 Hz, 3H). ^{13}C NMR (126 MHz, CD_2Cl_2) δ (ppm): 164.8, 162.8, 161.0, 155.2, 152.6, 151.7, 151.3, 149.8, 149.1, 147.1, 140.9, 139.5, 139.4, 139.2, 136.9, 128.9, 127.0, 125.8, 124.3, 124.1, 123.9, 118.3, 114.9, 114.2, 112.2, 99.5, 46.7, 32.1, 30.2, 29.5, 27.1, 22.9, 14.2. Anal. calcd (%) for $C_{42}H_{37}N_5PF_{10}Ir$, C 49.22, H 3.64, N 6.83; found, C 49.25, H 3.68, N 6.78.

2.4. Fabrication and Characterization of LEC Devices. LEC devices were fabricated using poly(3,4-ethylenedioxythiophene):poly styrenesulfonate (PEDOT:PSS) as the buffer layer and iridium complexes as light emitting layer materials. PEDOT:PSS (Clevios AI 4083) solutions were also used as hole conducting materials to smooth the anodic indium tin oxide (ITO) surfaces.[42] Prior to the fabrication process, ITO glass plates were cleaned in an ultrasonic bath containing mixed solvents such as ethanol, acetone, and isopropyl alcohol for 30 min followed by UV−ozone treatment for 20 min. The PEDOT:PSS solutions were then spin coated onto the ITO surfaces at 2000 rpm for 20 s and baked at 120 °C for 10 min. The active layer solutions were prepared separately in acetonitrile using 20 mg of the complexes (**1**−**6**) with a concentration of 0.022 M. The solutions were kept inside the shaking incubator for 24 h and then filtered using a 0.1 μm PTFE filter. These solutions were then spin coated onto the top of the ITO/PEDOT:PSS layer and subjected to an annealing process at 70 °C for

dx.doi.org/10.1021/am5058426 | ACS Appl. Mater. Interfaces XXXX, XXX, XXX−XXX

1 h in a vacuum oven. The samples were then transferred to a thermal evaporator where aluminum (100 nm) deposition was conducted using a shadow mask under high vacuum. The resulting devices exhibited the structure of ITO/PEDOT:PSS/iTMCs/Al. The electroluminescent properties of these devices were evaluated using Keithley characterization systems. The current density and luminance versus voltage sweeps were measured using a Keithley 2400 source meter and calibrated with a silicon photodiode. An Avantes luminance spectrometer was used to measure the EL spectrum and Commission Internationale de L'Eclairage (CIE) coordinates.

3. RESULTS AND DISCUSSION

3.1. Photophysical Properties. The room-temperature UV−vis absorption spectra of complexes **1**−**6** in acetonitrile are shown in Figure 1. The absorption spectra of complexes **1**, **3**, and **5** show similar absorption bands that vary from those of complexes **2**, **4**, and **6** and differ from one another according to the length of the alkyl chain on the ancillary ligand. However, complexes **1**−**6** all displayed broad and intense absorption bands in the UV region of the spectrum (200−350 nm). These bands were attributed to the spin-allowed ligand-centered (LC) $^1\pi-\pi^*$ transitions of both the cyclometalated and ancillary ligands. Weak absorption bands were observed starting at 360 nm and extending into the visible region, and they corresponded to the spin-allowed metal-to-ligand charge transfer (^{1}MLCT), spin-forbidden metal-to-ligand charge transfer (^{3}MLCT), ligand−to−ligand charge-transfer (^{3}LLCT and ^{1}LLCT), and ligand-centered (LC) $^3\pi-\pi^*$ transitions of the complexes.[49] The absorption spectra of complexes **2**, **4**, and **6** were significantly blue-shifted by approximately 20 nm compared to those of phenylpyridine complexes such as **1**, **3**, and **5**, because of the presence of electron withdrawing fluorine atoms on the cyclometalated ligands. Although different alkyl groups were present on the ancillary ligand, the ligand did not display any significant differences in the absorption properties of the complexes, indicating that the absorption spectra were independent of the alkyl chain length.

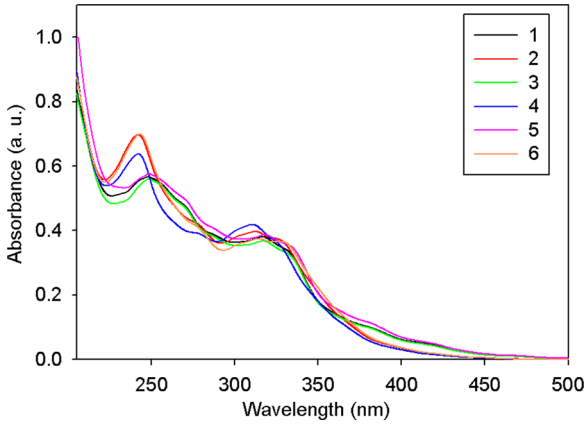

Figure 1. UV−vis absorption spectra of cationic iridium complexes **1**−**6** in acetonitrile at room temperature.

Figure 2 displays the PL emission spectra of complexes **1**−**6** in acetonitrile (10^{-5} M) at room temperature. The emission spectra of the complexes exhibited broad and featureless emission peaks for complexes **1**−**6**, which indicated that the emissive excited states have ^{3}MLCT or ^{3}LLCT characteristics instead of LC $^3\pi-\pi^*$ characteristics.[50,51] The photophysical characteristics of complexes **1**−**6** are summarized in Table 1. The emission spectra of complexes **1** (572 nm), **3** (579 nm), and **5** (576 nm) exhibited similar emission characteristics with yellow emission, despite three different sizes of alkyls groups being attached to the imidazole-based ancillary ligand. These results confirm that the addition of the alkyl groups with varying chain lengths do not affect the emission maxima of these complexes. Similar trends were also observed for complexes **2**, **4**, and **6** with emission maxima at 522, 527, and 526 nm, respectively, which correspond to green emission. The emission spectra of complexes **2**, **4**, and **6** were blue-shifted approximately 50 nm compared to those of complexes **1**, **3**, and **5**, because of the presence of electron withdrawing fluorine atoms on the cyclometalated ligands, which significantly affected the energy levels of these complexes. In addition, PL quantum yields (PLQYs) of complexes **1**−**6** were measured and show high quantum yields of 0.40−0.54 in acetonitrile solutions. Among the complexes, **5** exhibits higher PLQYs of 0.54, indicating that the rigidity of octyl group in the imidazole based ancillary ligand, which is beneficial for reducing nonradiative deactivation processes.

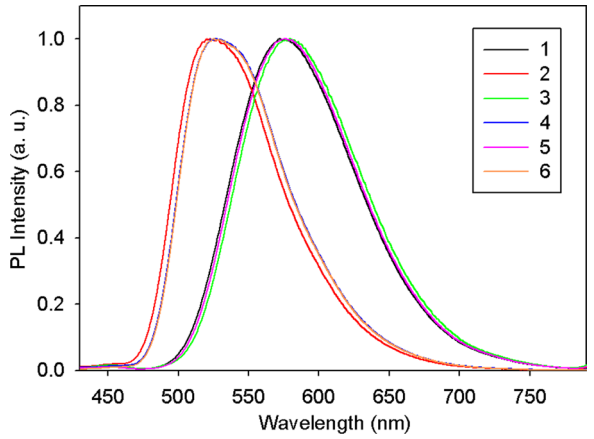

Figure 2. Photoluminescence (PL) emission spectra of cationic iridium complexes **1**−**6** in acetonitrile at room temperature.

3.2. Electrochemical Properties. The electrochemical properties of complexes **1**−**6** were evaluated by cyclic voltammetry and the redox potentials were measured versus ferrocenium/ferrocene (Fc^+/Fc) using 0.1 M $TBAPF_6$ in acetonitrile. The measured redox potentials are listed in Table 1. As shown in Figure 3, complexes **1**−**6** exhibited reversible oxidation and reduction processes in acetonitrile, attributed to the transportation of both holes and electrons, which are beneficial for the incorporation of these complexes into LECs.[22] Complexes **1**, **3**, and **5** show almost the same oxidation peaks with corresponding peak potentials of 1.18, 1.16, and 1.18 V, respectively, which can be attributed to the oxidation of Ir(III) to Ir(IV) with minor contributions from the cyclometalated ligand. Alternatively, the oxidation potentials of complexes **2**, **4**, and **6** are anodically shifted to 1.49, 1.49, and 1.51 V, respectively. The higher oxidation potentials of these complexes are attributed to the presence of electron withdrawing fluorine atoms that reduce the electron density around the iridium center and therefore inhibit the oxidation of complexes.[52,53] Similarly, the complexes exhibited reversible reduction peaks at −1.63 V (**1**), −1.53 V (**2**), −1.61 V (**3**), −1.56 V (**4**), −1.64 V (**5**), and −1.49 V (**6**) because of the reduction of the ancillary ligands. Additionally, each complex exhibited a peak at approximately −1.10 V that can be attributed to the reduction of the cyclometalated ligand. The

dx.doi.org/10.1021/am5058426 | ACS Appl. Mater. Interfaces XXXX, XXX, XXX−XXX

Table 1. Photophysical and Electrochemical Properties of Cationic Iridium Complexes 1−6

				electrochemical data		
complex	absorbance, λ (nm)	PL emission, λ_{max} (nm)	PL quantum yield (Φ_p)	E_{ox} (V)	E_{red} (V)	E_{gap}
1	248, 317, 385, 420	572	0.45	1.18	−1.63 −1.12	2.81
2	242, 275, 312, 400	522	0.40	1.49	−1.53 −1.05	3.02
3	249, 319, 383, 421	579	0.43	1.16	−1.61 −1.10	2.77
4	242, 276, 310, 397	527	0.41	1.49	−1.56 −1.10	3.05
5	249, 319, 381, 420	576	0.54	1.18	−1.64 −1.11	2.82
6	242, 276, 312, 403	526	0.50	1.51	−1.49 −1.02	3.0

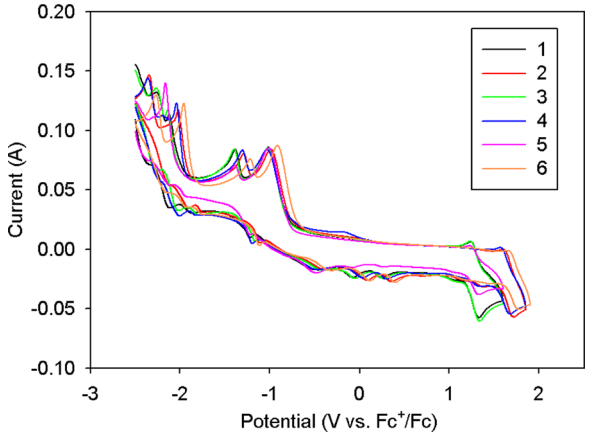

Figure 3. Cyclic voltammograms of cationic iridium complexes **1**−**6** in acetonitrile (10^{-3} M). The potentials were recorded versus Fc^+/Fc (Fc is ferrocene).

HOMO and LUMO energies and the electrochemical energy gaps (E_{gap}) of the complexes were calculated from their corresponding oxidation and reduction potentials. The calculated HOMO−LUMO energy gaps of the complexes were 2.81 V (**1**), 3.02 V (**2**), 2.77 V (**3**), 3.05 V (**4**), 2.82 V (**5**), and 3.0 V (**6**). The E_{gap} of complexes **1**, **3**, and **5** were similar, which indicates the alkyl chain lengths do not significantly affect the electrochemical properties of the complexes, as seen in complexes **2**, **4**, and **6**. However, a large difference in energy gaps was observed between these two classes of complexes, arising from the electron withdrawing fluorine atoms, which caused significant HOMO stabilization compared to that in complexes **1**, **3**, and **5**.

3.3. Density Functional Theory (DFT) Calculations. To gain insight into the photophysical and electrochemical properties of the iridium complexes, we performed DFT calculations using the Gaussian 09 suite of programs. The geometries of the complexes were optimized by using the B3LYP functional, and the Ir atom was treated by the LANL2DZ basis set, while all other atoms were treated by the 6-31G(d,p) basis set. The energy and electron density contours calculated for the HOMO and the LUMO of complexes **1**−**5** in the ground state are displayed in Figure 4. As shown in Figure 4, the HOMOs of all complexes were located on the t_{2g} orbitals of iridium ion and phenyl π orbitals of cyclometalated ligands, which were consistent with other previously reported complexes.[35,47] However, complexes **2** and

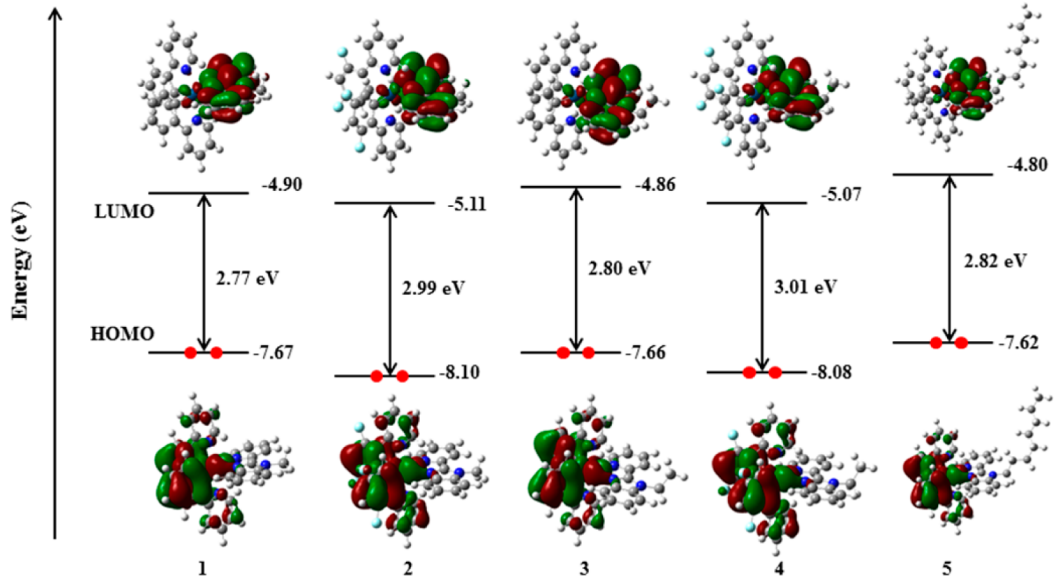

Figure 4. Energy and electron density contours calculated for the HOMOs and the LUMOs of complexes **1**−**5** in the ground state.

dx.doi.org/10.1021/am5058426 | ACS Appl. Mater. Interfaces XXXX, XXX, XXX−XXX

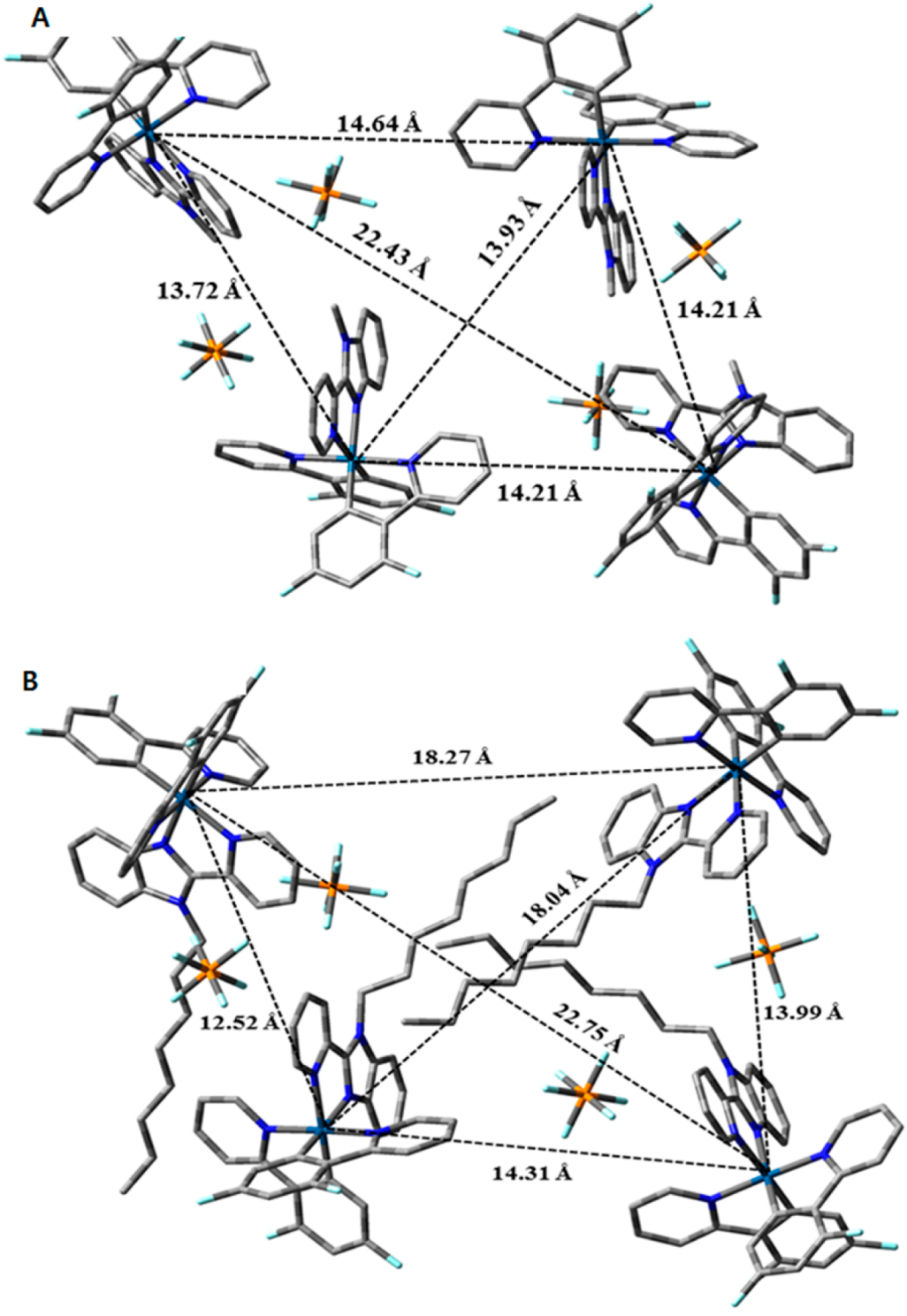

Figure 5. Arrangement and intermolecular distance of optimized packing structure of four molecules of complexes (A) **2** and (B) **6** in tetragonal form.

4 exhibited a significant stabilization of the HOMO by lowering its energy due to their electron withdrawing fluorine atoms. In contrast to HOMO, the electron density contribution of the LUMOs of all complexes lies on the π^* orbital of the ancillary ligand. The LUMO+1 were calculated for all complexes, which are slightly above the LUMO orbitals and exhibited similar electron density distributions as the LUMO orbitals. However, the LUMO+2 orbitals of all complexes differed from the LUMO orbitals, which were located on the t_{2g} orbitals of iridium ion and phenyl π orbitals of cyclometalated ligands. The HOMO−LUMO energy gaps were calculated for the series of complexes and exhibited the same trend that was observed in the electrochemical energy gaps: **1** (2.77 eV), **2** (2.99 eV), **3** (2.80 eV), **4** (3.01 eV), and **5** (2.82 eV). These results confirm that the alkyl chain length does not significantly increase the energy gaps of the complexes; however, a blue-shift in energy levels was observed only by replacing the cyclometalated ligands from ppy to dfppy.

dx.doi.org/10.1021/am5058426 | *ACS Appl. Mater. Interfaces* XXXX, XXX, XXX−XXX

To study the intermolecular interactions between iridium complexes having varying chain lengths, we performed theoretical calculations using semiempirical method (PM6 method). The interaction energies were measured for the optimized structures and were found to decrease from methyl to octyl group with energies of 56.68 kJ/mol for the complex having methyl side chain, 55.84 kJ/mol for ethyl side chain, and 37.6 kJ/mol for octyl side chain. This indicates the decreased intermolecular interaction for the complexes containing octyl side chain. The intermolecular distances for the optimized geometry were also calculated. The intermolecular distance of optimized packing structure of the tetramer for both methyl and octyl substituted complexes are shown in Figure 5. In the structures, the Ir atoms are at the corners of a rhombus for methyl substituted compound (complex **2**) and at the corners of a trapezium for the octyl substituted compound (complex **6**). In the case of complex **6**, the Ir−Ir distances between diagonal molecules are 18.04 and 22.75 Å, which has greatly increased compared to that of complex **2** (13.93 and 22.43 Å, respectively) indicating the reduced steric interactions of the complex containing octyl side chains.

3.4. Electroluminescent Properties of LECs. LECs were fabricated for studying the effects of the alkyl chain length on the electroluminescent properties of complexes **1**−**6**. The resulting devices had a structure of ITO/PEDOT:PSS(40 nm)/iTMC(75 nm)/Al. Figure 6 displays the EL spectra of the

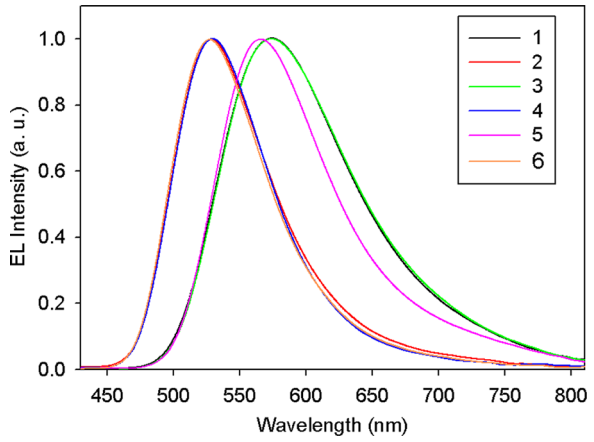

Figure 6. Electroluminescence (EL) spectra of the ITO/PEDOT:PSS/cationic iridium complexes **1**−**6**/Al.

LECs incorporating the cationic iridium complexes **1**−**6**, which produced broad and unstructured emission peaks that resembled the PL spectra in acetonitrile. The detailed electrical characteristics of the complexes are shown in Table 2. LECs

Table 2. Electrical Characteristics of the LECs Containing Cationic Iridium Complexes 1−6.

complex	maximum luminance (cd m^{-2})	maximum current density (mA cm^{-2})	maximum current efficiency (cd A^{-1})	EL λ_{max} (nm)	CIE coordinates
1	2842	263.94	1.48	575	(0.49, 0.50)
2	1520	135.48	1.12	527	(0.33, 0.60)
3	2933	253.98	1.23	574	(0.49, 0.50)
4	1642	196.71	0.83	529	(0.33,0.59)
5	7309	243.13	3.85	566	(0.47, 0.52)
6	3112	248.99	2.16	527	(0.32, 0.61)

incorporating complexes **1** and **3** exhibited similar emission properties with the maximum emission at 575 nm; however, a blue shift in the emission spectra was observed for complex **5** (which contained an octyl side group) due to the reduced intermolecular interaction compared to complexes **1** and **3**.[35] The CIE coordinates of complexes **1**, **3**, and **5** were (0.49, 0.50), (0.49, 0.50), and (0.47, 0.52), respectively, and corresponded to yellow emission. However, the complexes containing dfppy cyclometalated ligands significantly shifted the emission spectra to the shorter wavelength region. LECs based on these complexes emit green light (527 nm) with CIE coordinates of (0.33, 0.60), (0.33, 0.59), and (0.32, 0.61) for complex **2**, **4**, and **6**, respectively. The blue shift in the emission spectra of these complexes resulted from the electron withdrawing fluorine atoms that more effectively stabilized the HOMO and therefore shifted the emission color to a shorter wavelength region.

To determine any additional effects of alkyl chain length, we evaluated the electrical properties of the LECs. Figure 7

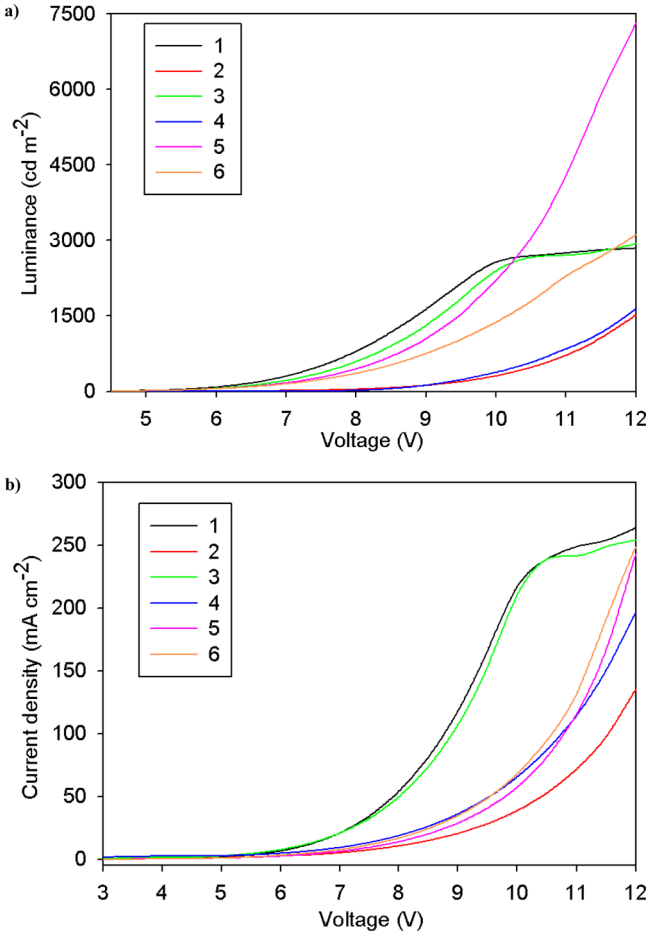

Figure 7. (a) Luminance and (b) current density versus voltage curves of ITO/PEDOT:PSS/cationic iridium complexes **1**−**6**/Al.

displays the luminance and current density versus the voltage curves of the LEC devices with a sweep rate of 0.5 V/sec. As shown in Figure 7, the luminance and current density of the devices containing cationic iridium complexes slowly increased as the voltage increased, which is a typical characteristic of LECs.[1,19] The stagnant nature of the LECs results from the slow mobility of counterions toward the electrode surface,

dx.doi.org/10.1021/am5058426 | ACS Appl. Mater. Interfaces XXXX, XXX, XXX−XXX

delayed carrier injection, and recombination. However, a gradual increase in luminance and current density was observed after a specific voltage was obtained, and the system subsequently reached a maximum intensity. It is important to note that the luminance of all devices increased as the chain length increased, which is due to the decreased intermolecular interactions between the molecules. When we increased the chain length from the methyl group to the octyl group, a prominent increase in luminance intensity was observed for complexes containing octyl groups as a result of the decreased intermolecular interaction between the two complex molecules. Consequently, an increased carrier injection and recombination occurred as the voltage increased. Additionally, the 2-phenylpyridine-based complex (**5**) exhibited better performances than the corresponding difluorophenylpyridine complexes because of the lower charge injection barrier of complex **5**, which promoted a more balanced charge recombination compared to that of complex **6**.

Detailed device performances are shown in Table 2. LECs incorporating complex **1** resulted in a luminance of 2842 cd m^{-2}, a current density of 263.94 mA cm^{-2}, and a peak current efficiency of 1.48 cd A^{-1}. However, the device containing **2** exhibited a luminance, current density, and current efficiency of 1520 cd m^{-2}, 135.48 mA cm^{-2}, and 1.12 cd A^{-1}, respectively. Similarly, the performance of the device containing **3** or **4** exhibited enhanced performances with a luminance of 2933 and 1642 cd m^{-2}, respectively. However, the current efficiencies of the LECs based on these complexes were lower than that of **1** and **2** because of the higher current density generated for these complexes. When moving from the methyl group to the octyl group, the luminance increased 2-fold with current efficiencies of 3.85 and 2.16 cd A^{-1} for **5** and **6**, respectively. Our results suggest that the alkyl chain lengths have a significant impact on the electroluminescent properties of LECs, which reduce the intermolecular interactions between the molecules, therefore greatly enhancing the device performance of systems containing compounds with longer chains compared to that of systems containing compounds with shorter alkyl chains.

4. CONCLUSIONS

Six cationic iridium complexes with imidazole-based ancillary ligands containing various alkyl chain lengths were synthesized and incorporated into LEC devices, and the effects of chain length on the electroluminescent properties of the devices were evaluated. LECs based on these complexes resulted in yellow electroluminescence when utilizing complexes containing the ppy cyclometalated ligand (complexes **1**, **3**, and **5**). However, green emission was produced from the complexes containing dfppy cyclometalated ligands (complexes **2**, **4**, and **6**). Although the chain length did not influence the color of the complexes, it did play a pivotal role in the device performance by reducing the intermolecular interactions between iridium molecules. Consequently, a very high luminance of 7309 cd m^{-2}, current density of 243.13 mA cm^{-2}, and current efficiency of 3.85 cd A^{-1} were observed for LECs containing complex **5**.

AUTHOR INFORMATION

Corresponding Author

*Tel.: +8251 510 2396. Fax: +8251 512 8634. E-mail: choe@pusan.ac.kr.

Notes

The authors declare no competing financial interest.

ACKNOWLEDGMENTS

This work was supported by the Basic Science Research Program through the National Research Foundation (NRF) of Korea funded by the Ministry of Education, Science, and Technology (NRF-2013R1A1A4A03009795), and the BK 21 PLUS Centre for Advanced Chemical Technology (21A20131800002), Republic of Korea.

REFERENCES

(1) Pei, Q.; Yu, G.; Zhang, C.; Yang, Y.; Heeger, A. J. Polymer Light-Emitting Electrochemical Cells. *Science* **1995**, *269*, 1086−1088.

(2) Sun, Q. J.; Li, Y. F.; Pei, Q. B. Polymer Light-Emitting Electrochemical Cells for High-Efficiency Low-Voltage Electroluminescent Devices. *J. Disp. Technol.* **2007**, *3*, 211−224.

(3) Lee, J. K.; Yoo, D. S.; Handy, E. S.; Rubner, M. F. Thin Film Light Emitting Devices from an Electroluminescent Ruthenium Complex. *Appl. Phys. Lett.* **1996**, *69*, 1686−1688.

(4) Slinker, J.; Bernards, D.; Houston, P. L.; Abruna, H. D.; Bernhard, S.; Malliaras, G. G. Solid-State Electroluminescent Devices Based on Transition Metal Complexes. *Chem. Commun.* **2003**, *19*, 2392−2399.

(5) Slinker, J. D.; Rivnay, J.; Moskowitz, J. S.; Parker, J. B.; Bernhard, S.; Abruna, H. D.; Malliaras, G. G. Electroluminescent Devices from Ionic Transition Metal Complexes. *J. Mater. Chem.* **2007**, *17*, 2976−2988.

(6) deMello, J. C.; Tessler, N.; Graham, S. C.; Friend, R. H. Ionic Space-Charge Effects in Polymer Light-Emitting Diodes. *Phys. Rev. B* **1998**, *57*, 12951−12963.

(7) Rudmann, H.; Rubner, M. F. Single Layer Light-Emitting Devices with High Efficiency and Long Lifetime Based on Tris(2,2′-bipyridyl)ruthenium(II) Hexafluorophosphate. *J. Appl. Phys.* **2001**, *90*, 4338−4345.

(8) Gao, F. G.; Bard, A. J. Solid-State Organic Light-Emitting Diodes Based on Tris(2,2′-bipyridine)ruthenium(II) Complexes. *J. Am. Chem. Soc.* **2000**, *122*, 7426−7427.

(9) Bolink, H. J.; Cappelli, L.; Coronado, E.; Gavina, P. Observation of Electroluminescence at Room Temperature from a Ruthenium(II) Bis-Terpyridine Complex and Its Use for Preparing Light-Emitting Electrochemical Cells. *Inorg. Chem.* **2005**, *44*, 5966−5968.

(10) Kalyuzhny, G.; Buda, M.; McNeill, J.; Barbara, P.; Bard, A. J. Stability of Thin-Film Solid-State Electroluminescent Devices Based on Tris(2,2′-bipyridine)ruthenium(II) Complexes. *J. Am. Chem. Soc.* **2003**, *125*, 6272−6283.

(11) Soltzberg, L. J.; Slinker, J. D.; Flores-Torres, S.; Bernards, D. A.; Malliaras, G. G.; Abruña, H. D.; Kim, J. S.; Friend, R. H.; Kaplan, M. D.; Goldberg, V. Identification of a Quenching Species in Ruthenium Tris-Bipyridine Electroluminescent Devices. *J. Am. Chem. Soc.* **2006**, *128*, 7761−7764.

(12) Lyons, C. H.; Abbas, E. D.; Lee, J. K.; Rubner, M. F. Solid-State Light-Emitting Devices Based on the Trischelated Ruthenium(II) Complex. 1. Thin Film Blends with Poly(ethylene oxide). *J. Am. Chem. Soc.* **1998**, *120*, 12100−12107.

(13) Gao, F. G.; Bard, A. J. High-Brightness and Low-Voltage Light-Emitting Devices Based on Trischelated Ruthenium(II) and Tris(2,2′-bipyridine)osmium(II) Emitter Layers and Low Melting Point Alloy Cathode Contacts. *Chem. Mater.* **2002**, *14*, 3465−3470.

(14) Hosseini, A. R.; Koh, C. Y.; Slinker, J. D.; Torres, S. F.; Abruna, H. D.; Malliaras, G. G. Addition of a Phosphorescent Dopant in Electroluminescent Devices from Ionic Transition Metal Complexes. *Chem. Mater.* **2005**, *17*, 6114−6116.

(15) Armaroli, N.; Accorsi, G.; Holler, M.; Moudam, O.; Nierengarten, J. F.; Zhou, Z.; Wegh, R. T.; Welter, R. Highly Luminescent Cu^{I} Complexes for Light-Emitting Electrochemical Cells. *Adv. Mater.* **2006**, *18*, 1313−1316.

(16) Kalsani, V.; Schmittel, M.; Listorti, A.; Accorsi, G.; Armaroli, N. Novel Phenanthroline Ligands and Their Kinetically Locked Copper-(I) Complexes with Unexpected Photophysical Properties. *Inorg. Chem.* **2006**, *45*, 2061−2067.

(17) Zhang, Q. S.; Zhou, Q. G.; Cheng, Y. X.; Wang, L. X.; Ma, D. G.; Jing, X. B.; Wang, F. S. Highly Efficient Electroluminescence from Green-Light-Emitting Electrochemical Cells Based on Cu^{I} Complexes. *Adv. Funct. Mater.* **2006**, *16*, 1203−1208.
(18) Felici, M.; Contreras-Carballada, P.; Smits, J. M. M.; Nolte, R. J. M.; Williams, R. M.; De Cola, L.; Feiters, M. C. Cationic Heteroleptic Cyclometalated $Iridium^{III}$ Complexes Containing Phenyl-Triazole and Triazole-Pyridine Clicked Ligands. *Molecules* **2010**, *15*, 2039−2059.
(19) Slinker, J. D.; Gorodetsky, A. A.; Lowry, M. S.; Wang, J. J.; Parker, S.; Rohl, R.; Bernhard, S.; Malliaras, G. G. Efficient Yellow Electroluminescence from a Single Layer of a Cyclometalated Iridium Complex. *J. Am. Chem. Soc.* **2004**, *126*, 2763−2767.
(20) Costa, R. D.; Ortí, E.; Tordera, D.; Pertegás, A.; Bolink, H. J.; Graber, S.; Housecroft, C. E.; Sachno, L.; Neuburger, M.; Constable, E. C. Stable and Efficient Solid-State Light-Emitting Electrochemical Cells Based on a Series of Hydrophobic Iridium Complexes. *Adv. Energy Mater.* **2011**, *1*, 282−290.
(21) He, L.; Duan, L.; Qiao, J.; Zhang, D.; Wang, L.; Qiu, Y. Enhanced Stability of Blue-Green Light-Emitting Electrochemical Cells Based on a Cationic Iridium Complex with 2-(1-Phenyl-1*H*-pyrazol-3-yl)pyridine as the Ancillary Ligand. *Chem. Commun.* **2011**, *47*, 6467−6469.
(22) Chen, B.; Li, Y.; Yang, W.; Luo, W.; Wu, H. Efficient Sky-Blue and Blue-Green Light-Emitting Electrochemical Cells Based on Cationic Iridium Complexes Using 1,2,4-Triazole-pyridine as the Ancillary Ligand with Cyanogen Group in Alkyl Chain. *Org. Electron.* **2011**, *12*, 766−773.
(23) Sun, L.; Galan, A.; Ladouceur, S.; Slinker, J. D.; Colman, E. Z. High Stability Light-Emitting Electrochemical Cells from Cationic Iridium Complexes with Bulky 5,5′ Substituents. *J. Mater. Chem.* **2011**, *21*, 18083−18088.
(24) Zhang, J.; Zhou, L.; Al-Attar, H. A.; Shao, K.; Wang, L.; Zhu, D.; Su, Z.; Bryce, M. R.; Monkman, A. P. Efficient Light-Emitting Electrochemical Cells (LECs) Based on Ionic Iridium(III) Complexes with 1,3,4-Oxadiazole Ligands. *Adv. Funct. Mater.* **2013**, *23*, 4667−4677.
(25) Kessler, F.; Costa, R. D.; Censo, D. D.; Scopelliti, R.; Ortí, E.; Bolink, H. J.; Meier, S.; Sarfert, W.; Grätzel, M.; Nazeeruddin, M. K.; Baranoff, E. Near-UV to Red-Emitting Charged Bis-Cyclometallated Iridium(III) Complexes for Light-Emitting Electrochemical Cells. *Dalton Trans.* **2012**, *41*, 180−191.
(26) Sunesh, C. D.; Sunseong, O.; Chandran, M.; Moon, D.; Choe, Y. Effect of Ionic Liquids on the Electroluminescence of Yellowish-Green Light-Emitting Electrochemical Cells Using Bis(2-(2,4-difluorophenyl)pyridine)4,7-diphenyl-1,10-phenanthroline-iridium-(III) Hexafluorophosphate. *Mater. Chem. Phys.* **2012**, *136*, 173−178.
(27) Tordera, D.; Pertegas, A.; Shavaleev, N. M.; Scopelliti, R.; Ortí, E.; Bolink, H. J.; Baranoff, E.; Gratzel, M.; Nazeeruddin, M. K. Efficient Orange Light-Emitting Electrochemical Cells. *J. Mater. Chem.* **2012**, *22*, 19264−19268.
(28) Sunesh, C. D.; Mathai, G.; Cho, Y. R.; Choe, Y. Optoelectronic Properties of Green and Yellow Light-Emitting Electrochemical Cells Based on Cationic Iridium Complexes. *Polyhedron* **2013**, *57*, 77−82.
(29) Costa, R. D.; Ortí, E.; Bolink, H. J.; Graber, S.; Housecroft, C. E.; Constable, E. C. Light-Emitting Electrochemical Cells Based on a Supramolecularly-Caged Phenanthroline-Based Iridium Complex. *Chem. Commun.* **2011**, *47*, 3207−3209.
(30) Sunesh, C. D.; Chandran, M.; Mathai, G.; Choe, Y. Highly Luminescent Yellow and Yellowish-Green Light-Emitting Electrochemical Cells Based on Cationic Iridium Complexes with Phenanthroline Based Ancillary Ligands. *Opt. Mater.* **2013**, *35*, 407−413.
(31) Meier, S. B.; Sarfert, W.; Junquera-Herńandez, J. M.; Delgado, M.; Tordera, D.; Orti, E.; Bolink, H. J.; Kessler, F.; Scopelliti, R.; Gŕatzel, M.; Nazeeruddind, M. K.; Baranoff, E. A Deep-Blue Emitting Charged Bis-Cyclometallated Iridium(III) Complex for Light-Emitting Electrochemical Cells. *J. Mater. Chem. C* **2013**, *1*, 58−68.
(32) Chen, B.; Li, Y.; Chu, Y.; Zheng, A.; Feng, J.; Liu, Z.; Wu, H.; Yang, W. Highly Efficient Single-Layer Organic Light-Emitting Devices Using Cationic Iridium Complex as Host. *Org. Electron.* **2013**, *14*, 744−753.
(33) Sunesh, C. D.; Mathai, G.; Choe, Y. Green and Blue−Green Light-Emitting Electrochemical Cells Based on Cationic Iridium Complexes with 2-(4-Ethyl-2-pyridyl)-1*H*-Imidazole Ancillary Ligand. *Org. Electron.* **2014**, *15*, 667−674.
(34) Su, H.; Fang, F. C.; Hwu, T. Y.; Hsieh, H. H.; Chen, H. F.; Lee, G. H.; Peng, S. M.; Wong, K. T.; Wu, C. C. Highly Efficient Orange and Green Solid-State Light-Emitting Electrochemical Cells Based on Cationic Ir^{III} Complexes with Enhanced Steric Hindrance. *Adv. Funct. Mater.* **2007**, *17*, 1019−1027.
(35) He, L.; Qiao, J.; Duan, L.; Dong, G. F.; Zhang, D. Q.; Wang, L. D.; Qiu, Y. Toward Highly Efficient Solid-State White Light-Emitting Electrochemical Cells: Blue-Green to Red Emitting Cationic Iridium Complexes with Imidazole-Type Ancillary Ligands. *Adv. Funct. Mater.* **2009**, *19*, 2950−2960.
(36) Costa, R. D.; Orti, E.; Bolink, H. J.; Graber, S.; Schaffner, S.; Neuburger, M.; Housecroft, C. E.; Constable, E. C. Archetype Cationic Iridium Complexes and Their Use in Solid-State Light-Emitting Electrochemical Cells. *Adv. Funct. Mater.* **2009**, *19*, 3456−3463.
(37) Liao, C. T.; Chen, H. F.; Su, H. C.; Wong, K. T. Improving the Balance of Carrier Mobilities of Host−Guest Solid-State Light-Emitting Electrochemical Cells. *Phys. Chem. Chem. Phys.* **2012**, *14*, 1262−1269.
(38) Costa, R. D.; Cespedes-Guirao, F. J.; Orti, E.; Bolink, H. J.; Gierschner, J.; Fernandez-Lazaro, F.; Sastre-Santos, A. Efficient Deep-Red Light-Emitting Electrochemical Cells Based on a Perylenediimide−Iridium-Complex Dyad. *Chem. Commun.* **2009**, 3886−3888.
(39) Costa, R. D.; Fernandez, G.; Sanchez, L.; Martin, N.; Orti, E.; Bolink, H. J. Dumbbell-Shaped Dinuclear Iridium Complexes and Their Application to Light-Emitting Electrochemical Cells. *Chem.—Eur. J.* **2010**, *16*, 9855−9863.
(40) Liao, C. T.; Chen, H. F.; Su, H. C.; Wong, K. T. Tailoring Carrier Injection Efficiency to Improve the Carrier Balance of Solid-State Light-Emitting Electrochemical Cells. *Phys. Chem. Chem. Phys.* **2012**, *14*, 9774−9784.
(41) Su, H. C.; Lin, Y. H.; Chang, C. H.; Lin, H. W.; Wu, C. C.; Fang, F. C.; Chen, H. F.; Wong, K. T. Solid-State Light-Emitting Electrochemical Cells Employing Phosphor-Sensitized Fluorescence. *J. Mater. Chem.* **2010**, *20*, 5521−5526.
(42) Tamayo, A. B.; Garon, S.; Sajoto, T.; Djurovich, P. I.; Tsyba, I. M.; Bau, R.; Thompson, M. E. Cationic Bis-Cyclometalated Iridium-(III) Diimine Complexes and Their Use in Efficient Blue, Green, and Red Electroluminescent Devices. *Inorg. Chem.* **2005**, *44*, 8723−8732.
(43) Costa, R. D.; Orti, E.; Bolink, H. J.; Monti, F.; Accorsi, G.; Armaroli, N. Luminescent Ionic Transition-Metal Complexes for Light-Emitting Electrochemical Cells. *Angew. Chem., Int. Ed.* **2012**, *51*, 8178−8211.
(44) Hu, T.; He, L.; Duan, L.; Qiu, Y. Solid-State Light-Emitting Electrochemical Cells Based on Ionic Iridium(III) Complexes. *J. Mater. Chem.* **2012**, *22*, 4206−4215.
(45) Liu, Y.; Liu, M. S.; Jen, A. K.-Y. Synthesis and Characterization of a Novel and Highly Efficient Light-Emitting Polymer. *Acta Polym.* **1999**, *50*, 105−108.
(46) Hwang, S. W.; Chen, Y. Synthesis and Electrochemical and Optical Properties of Novel Poly(aryl ether)s with Isolated Carbazole and *p*-Quaterphenyl Chromophores. *Macromolecules* **2001**, *34*, 2981−2986.
(47) Nonoyama, M. Benzo[*h*]quinolin-10-yl-*N*-iridium(III) Complexes. *Bull. Chem. Soc. Jpn.* **1974**, *47*, 767−768.
(48) Sprouse, S.; King, K. A.; Spellane, P. J.; Watts, R. J. Photophysical Effects of Metal-Carbon σ bonds in Ortho-Metalated Complexes of Ir(III) and Rh(III). *J. Am. Chem. Soc.* **1984**, *106*, 6647−6653.
(49) He, L.; Duan, L.; Qiao, J.; Wang, R.; Wei, P.; Wang, L.; Qiu, Y. Blue-Emitting Cationic Iridium Complexes with 2-(1*H*-Pyrazol-1-yl)pyridine as the Ancillary Ligand for Efficient Light-Emitting Electrochemical Cells. *Adv. Funct. Mater.* **2008**, *18*, 2123−2131.

(50) Colombo, M. G.; Gudel, H. U. Synthesis and High-Resolution Optical Spectroscopy of Bis[2-(2-thienyl)pyridinato-C3,*N*′](2,2′-bipyridine)iridium(III). *Inorg. Chem.* **1993**, *32*, 3081−3087.
(51) Lowry, M. S.; Hudson, W. R.; Pascal, R. A.; Bernhard, S. Accelerated Luminophore Discovery Through Combinatorial Synthesis. *J. Am. Chem. Soc.* **2004**, *126*, 14129−14135.
(52) Adachi, C.; Kwong, R. C.; Djurovich, P.; Adamovich, V.; Baldo, M. A.; Thompson, M. E.; Forrest, S. R. Endothermic Energy Transfer: A Mechanism for Generating Very Efficient High-Energy Phosphorescent Emission in Organic Materials. *Appl. Phys. Lett.* **2001**, *79*, 2082−2084.
(53) Lowry, M. S.; Goldsmith, J. I.; Slinker, J. D.; Rohl, R.; Pascal, R. A.; Malliaras, G. G.; Bernhard, S. Single-Layer Electroluminescent Devices and Photoinduced Hydrogen Production from an Ionic Iridium(III) Complex. *Chem. Mater.* **2005**, *17*, 5712−5719.